Neuron
Article

A Conserved Switch in Sensory Processing Prepares Developing Neocortex for Vision

Matthew T. Colonnese,[1,*] Anna Kaminska,[2,3,4] Marat Minlebaev,[1] Mathieu Milh,[1] Bernard Bloem,[1] Sandra Lescure,[4,5,6] Guy Moriette,[4,5,6] Catherine Chiron,[3,4,7] Yehezkel Ben-Ari,[1] and Rustem Khazipov[1]
[1]INSERM, U901, INMED, Aix-Marseille Université, Faculté des Sciences, 13273 Marseille, France
[2]APHP, Groupe Hospitalier Cochin-Saint Vincent de Paul, Service de Physiologie et d'Exploration Fonctionnelle, 75014 Paris, France
[3]INSERM, U663, 75015 Paris, France
[4]Université Paris Descartes, Faculté de Médecine, 75006 Paris, France
[5]APHP, Groupe hospitalier Cochin, Service de Médecine néonatale de Port-Royal, 75014 Paris, France
[6]PremUP, 75006 Paris, France
[7]APHP, Necker-Enfants Malades Hospital, Department of Neuropediatrics, Centre de référence épilepsies rares, 75743 Paris, France
*Correspondence: colonnese@inmed.univ-mrs.fr
DOI 10.1016/j.neuron.2010.07.015

SUMMARY

Developing cortex generates endogenous activity that modulates the formation of functional units, but how this activity is altered to support mature function is poorly understood. Using recordings from the visual cortex of preterm human infants and neonatal rats, we report a "bursting" period of visual responsiveness during which the weak retinal output is amplified by endogenous network oscillations, enabling a primitive form of vision. This period ends shortly before delivery in humans and eye opening in rodents with an abrupt switch to the mature visual response. The switch is causally linked to the emergence of an activated state of continuous cortical activity dependent on the ascending neuromodulatory systems involved in arousal. This switch is sensory system specific but experience independent and also involves maturation of retinal processing. Thus, the early development of visual processing is governed by a conserved, intrinsic program that switches thalamocortical response properties in anticipation of patterned vision.

INTRODUCTION

Human infants show remarkable visual behavior, though poor acuity, soon after birth (Salapatek, 1986). The initial circuit development necessary for such behavior occurs prenatally, guided by an interaction between guidance molecules and spontaneous neuronal activity (Katz and Shatz, 1996; Rakic, 1976). As evidenced by studies in rodents and carnivores, in which the developmental template is shifted toward the postnatal period, the primary source of previsual activity is waves of spontaneous retinal activity, which influence map formation and afferent segregation in central visual structures (Huberman et al., 2008). Retinal waves are not simply transferred to cortex, but instead interact with immature network properties (Butts et al., 2007; Chiu and Weliky, 2001; Weliky and Katz, 1999) to generate developmentally unique patterns of network oscillations in cortex (Colonnese and Khazipov, 2010; Hanganu et al., 2006). It is currently unknown how these early network properties are regulated to support the development of visual information transfer necessary for both vision and synaptic plasticity beginning at eye opening (Li et al., 2008; Smith and Trachtenberg, 2007; White et al., 2001).

Profound changes occur at all levels of the visual system over this developmental period, each of which is likely to contribute to the development of visual processing. Light responses in retina mature in parallel with the downregulation of spontaneous waves (Demas et al., 2003; Wong et al., 1993; Tian and Copenhagen, 2003). During this time, thalamocortical and intracortical networks experience a progressive increase in the number and strength of synaptic connections and a change in neuronal excitability required for the generation of "mature" spontaneous activity and signal processing (Evrard and Ropert, 2009; McCormick et al., 1995; Golshani et al., 2009; Rochefort et al., 2009; Warren et al., 1994). In tandem, GABA, which patterns early neuronal networks via a depolarizing action on immature neurons, acquires its normal hyperpolarizing action (Ben-Ari et al., 2007), and neuromodulatory systems begin to differentiate cortical activity according to vigilance state (Seelke and Blumberg, 2010; Frank and Heller, 2003).

To determine how these developmental changes interact to shape sensory responses, we began with a detailed and progressive characterization of the early development of visual responses in preterm human neonates and nonanesthetized postnatal rats under comparable conditions. Behavioral and electrical responses to light develop prenatally in humans (Ellingson, 1960) and before eye opening in altricial animals (Ohshiro and Weliky, 2006; Krug et al., 2001). Using whole-field light flashes, the most salient stimulus for the obscured visual system (Akerman et al., 2002), we show that early visual responses are strongly amplified by the immature thalamocortical network. This enables a primitive form of vision despite weak retinal light responses and eyelid-obscured vision. We identify multiple visual system changes that are critical to the developmental transition to normal visual processing, including maturation of the retina and the emergence of a "continuous" mode of cortical

activity brought about by the development of cortical connections, as well as modulation of thalamocortical circuits by brainstem neuromodulatory systems.

RESULTS

Three Periods of Early Visual Development in the Rat

We made extracellular recordings from primary visual cortex of un-anesthetized, head restrained rats between postnatal (P) day 5 and P19 in order to observe alterations in the visual responses evoked by whole field light flashes (100 ms). To characterize evoked potentials across the complete frequency spectrum, we first used direct current coupled recordings of the local field potential and multiple-unit activity (MUA) in layer (L)4. We observed three distinct periods (Figure 1) we call "*Physiological blindness of immaturity*," "*Bursting*," and "*Acuity*."

(1) *Physiological blindness of immaturity* (≤P7): Light flashes of any intensity or duration failed to evoke a cortical response in this age group (n = 8; Figure 1B). Despite this, the visual cortex was spontaneously active, with retinal wave-driven spontaneous bursts of rhythmic activation nested within slow negative waves, which have been previously termed spindle-bursts, slow activity transients, or delta brushes (Hanganu et al., 2006; Colonnese and Khazipov, 2010). Spontaneous activity was separated by long-lasting (up to tens of seconds) down states during both waking and sleep.

(2) *Bursting period* (P8–11): At P8, light responsiveness emerged and light flashes reliably produced complex large-amplitude responses consisting of multiple slow-waves that grouped high-frequency oscillations lasting 1–3 s (Figures 1C and 1D). The response was typically composed of two events: (1) an "initial response" that began 150–400 ms (265 ± 88 ms [mean ± SD], n = 11 rats) after stimulation and consisted of field potential oscillations in the high beta and gamma bands (20 – 45 Hz; mean peak frequency 35.0 ± 6 Hz) culminating in a large negative wave and a burst of multiple-unit activity (MUA; mean duration 66.3 ± 22.0 ms; the total mean duration of the initial response was 203.6 ± 31 ms) and (2) a second event that occurred between 500–1200 ms after stimulation (mean time to peak 782 ± 155 ms) and consisted of a delta-band negative wave (mean duration 528 ± 160 ms) containing alpha/beta oscillations (8–30 Hz; mean peak frequency 20.5 ± 3.5 Hz). These two components resembled previously described oscillatory patterns in immature cortex, "gamma-bursts" (Yang et al., 2009; Seelke and Blumberg, 2010) and "spindle bursts" or "delta brushes" (Khazipov et al., 2004), respectively. The involvement of a stochastic process in the generation of evoked delta brushes was suggested by the significant variation in their delay, amplitude, and appearance between trials (Figure 1D). Interestingly, visual responses did not depend on the duration of the light flash and long duration light exposures (>30 s) caused similar visual responses both when the light was turned on and when it was extinguished (not shown). In vivo patch-clamp recordings revealed that both the initial response and evoked delta brush were composed of multiple synaptic glutamatergic and GABAergic currents tightly correlated to the field potential activity (see Figure S1 available online). These recordings also confirmed the separation of the initial response and evoked delta brush, which were divided by short periods of suppressed synaptic activity. Spontaneous activity at these ages remained discontinuous and poorly modulated by vigilance state.

(3) *Acuity period* (>P12): Starting on P12, 2 days before eye opening, light-evoked oscillations and slow-waves were no longer observed. In their place we observed a single negative visual evoked potential (VEP; mean duration 29.9 ± 12.7 ms, n = 10 P12–19 rats) associated with MUA but little oscillatory activity (Figure 1E). In contrast to earlier events, but like adult visual responses, the VEP was consistent in delay and appearance from trial to trial (Figure 1F). In vivo whole-cell recording showed that the shorter VEP was composed of a similarly restricted pattern of glutamatergic and GABAergic synaptic currents (Figure S1). Spontaneous activity as these ages became more continuous, with more frequent but smaller bursts, and began to display a greater diversity of oscillatory patterns and dependence on behavioral state.

We quantified the visual responses in 2 day increments using three parameters (Figure 1G): (1) The evoked potential, (2) time-spectral analysis between 5 and 50 Hz, and (3) rate of MUA (n = 5–6 rats per 2 day period; total 21 rats). P8–9 and P10–11 animals both showed long duration, high amplitude evoked potentials, as well as beta band oscillations in the second following stimulation. During the initial response, the MUA time-course was poorly time-locked to the stimulus at these ages and was elevated for an extended time following stimulation. Interestingly, an adult-like visual response, including a shortened average evoked potential and no evoked oscillations or extended MUA, was observed by P12–13, before eye opening, and these parameters were not subsequently altered (P14–15).

We quantified the role of vigilance states in the regulation of the visual response in a subset of animals (Figure 2). During the bursting period no significant differences were observed between wakefulness and sleep (n = 5 P10–11). During the acuity period, however, we observed state-dependent modulation of evoked activity. During sleep a second burst of MUA occurred following a brief suppression of ongoing activity (n = 4 P13–14). This burst occurred with a delay of 200–800 ms, primarily during quiet sleep (Figure 1F, asterisk, and Figure 2B) and was reminiscent of the k-complex, evoked by light during sleep (Amzica and Steriade, 1998). Unlike evoked delta brushes, triggered k complexes in visual cortex were not modality specific and could be evoked by sound or touch (Figure 2B). While occurring with the same delay as evoked delta-brushes, these bursts did not evidence their characteristic rapid oscillations or large amplitude slow wave (Figure 2C). Thus modulation of visual response by vigilance state develops only with the acuity period.

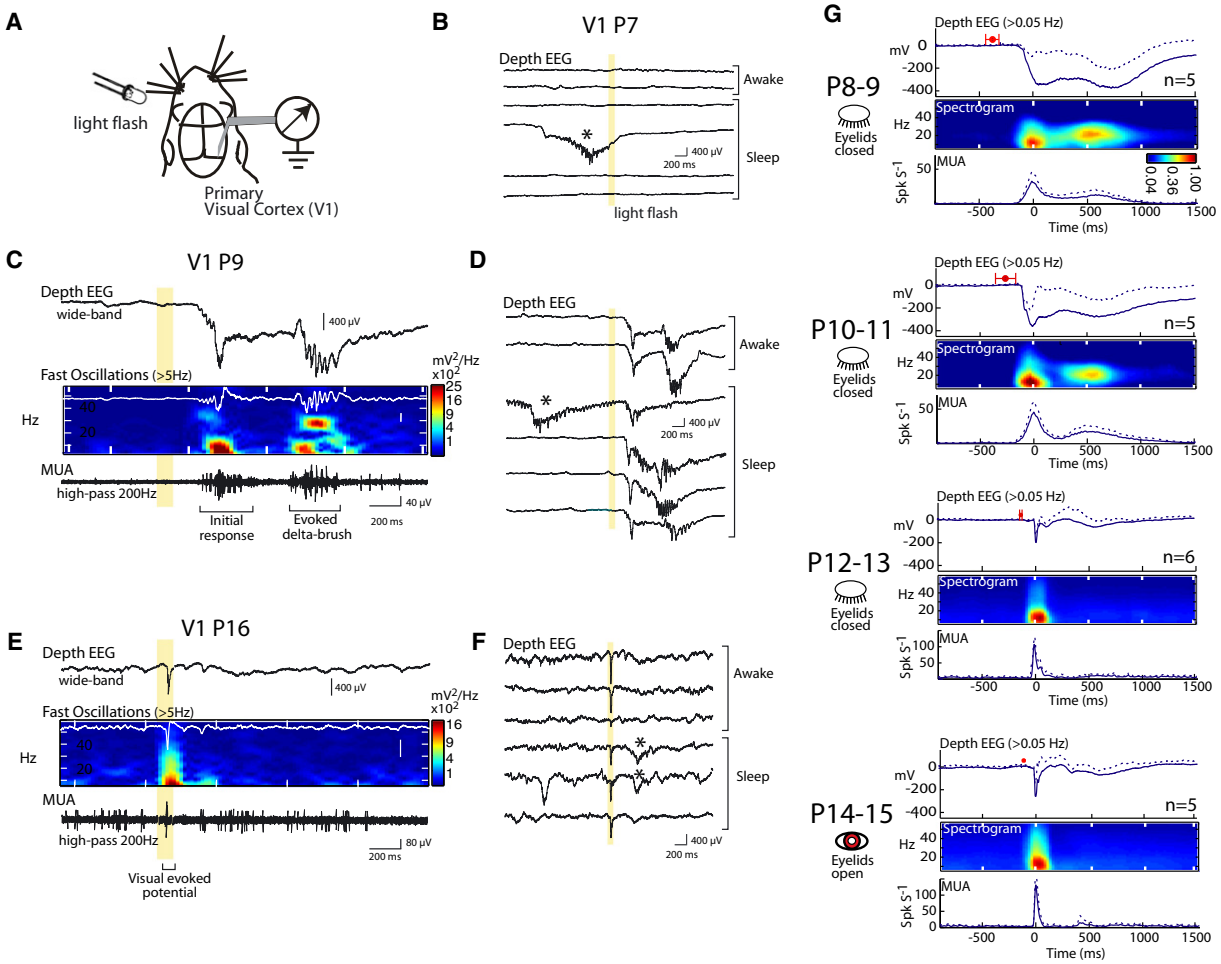

Figure 1. Three Periods in the Early Development of Visual Processing in the Rat

(A) Experimental setup. Primary visual cortex (V1) responses to 100 ms whole-field light flashes were recorded in head-fixed, unanesthetized rat pups between postnatal days (P)5 and P19 using extracellular direct current coupled recordings (band pass 0–5000 Hz) from L4.

(B) "Light blind" period (P7 and younger). Light flashes (yellow box) never evoked responses. A spontaneous delta brush is marked by asterisk.

(C and D) "Light-evoked bursting" period (P8–11). Flashes of light evoked long-duration, high-amplitude slow waves that were typically composed of two distinct poles; an "initial response" followed by an "evoked delta brush." Both waves contained rapid field potential oscillations. (C) Frequency decomposition of a single flash-evoked response from a P9 rat. Top trace is the raw depth EEG signal. In the middle the time series spectrogram, calculated for a 200 ms moving window from the high-pass filtered trace (white, HP > 2 Hz), reveals higher frequency components of the signal. The bottom trace shows the multiunit activity (MUA) in a high-pass filtered (>200 Hz) trace. Note that action potentials are specifically associated with the troughs of high-frequency oscillations. (D) Responses from the same animal in different awareness states.

(E and F) "Acuity" period (P12 and onward). Light flashes evoked adult-like visual evoked potentials (VEP), without delta brushes. (E) Frequency decomposition of single flash evoked response from a P16 rat. Note that the elevated power at multiple frequencies is due to the 200 ms integration window and to multiple frequencies intrinsic to the singular VEP. (F) Example traces as (D). During sleep, evoked bursts resembling the k complex were observed following light flashes (asterisk; see also Figure 2).

(G) Population average time-course of flash evoked responses in 2-day intervals. All time courses are aligned to the peak MUA rate for each animal (t = 0 s); the time of the light flash is shown as the red circle (±SD) above. For each panel, top trace is an average depth EEG signal (dotted line = SD); middle panel is an average time series spectrogram (proportion of peak frequency power 5–50 Hz) and bottom graph is an average rate of MUA calculated with a 20 ms sliding window (dotted line = SD). Note that switch from bursting to acuity response occurs before eye opening.

See Figure S1.

We were intrigued by the fact that such a striking developmental reduction in visual response has not been previously reported (Chapman and Stryker, 1993; Krug et al., 2001). Since anaesthetized animals were used in earlier studies, we determined the effects of isoflurane (0.3%–1%) on the responses. As shown in Figure S1, even very low doses (0.3%–1%) strongly suppressed the visual response in young rats. Other anesthetics including urethane (>0.8 g/kg, n = 5), ketamine (50 mg/kg, n = 7), and buprenophine (0.04 mg/kg, n = 3) similarly suppressed bursting responses.

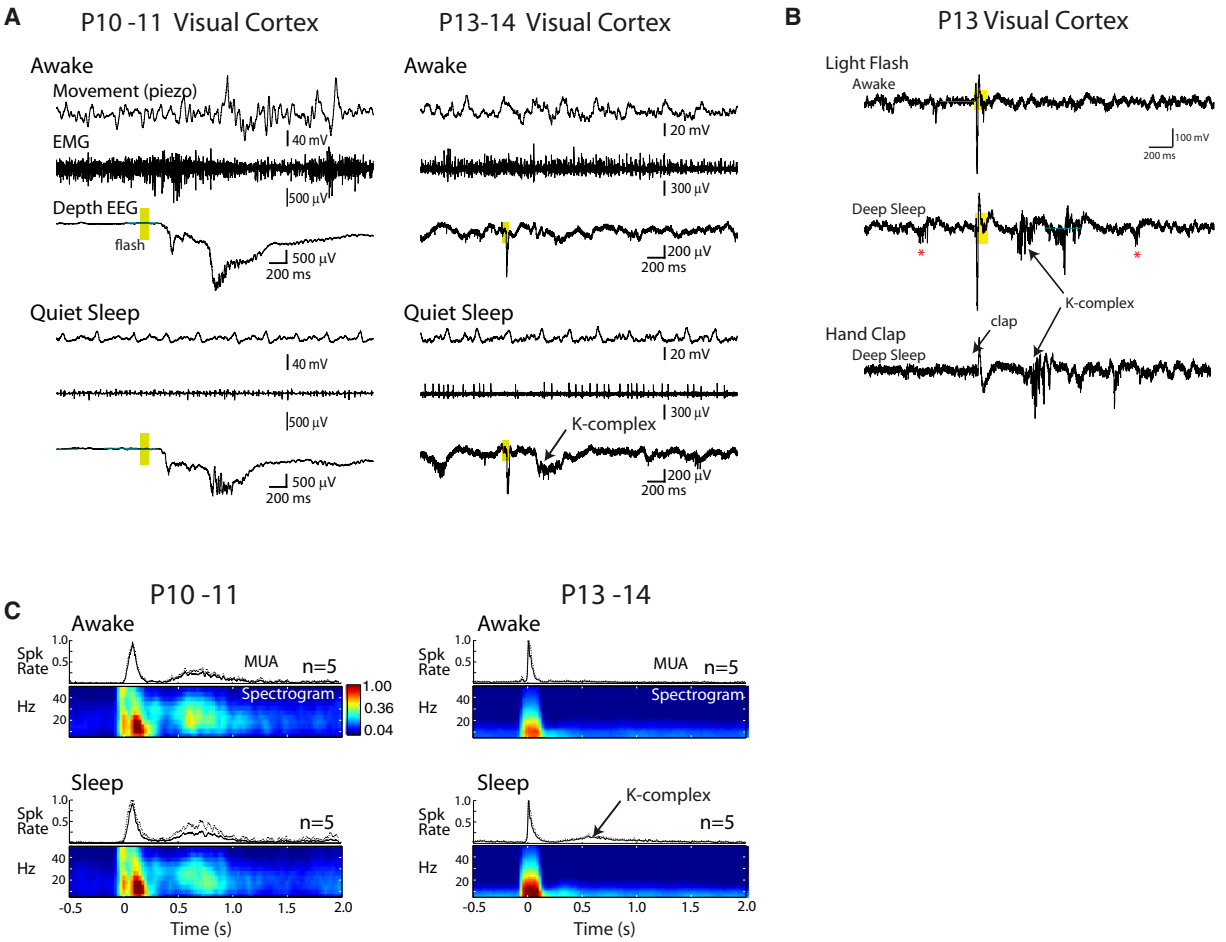

Figure 2. State Dependence of Light-Evoked Responses Develops after the Switch

(A) Example of evoked responses in different arousal states in V1. Simultaneous monitoring of EMG and movement was used to determine vigilance state. Visual responses were not modulated by vigilance state during the bursting period. During the acuity period light flashes evoked a singular sharp potential in all states, but during quiet sleep bursts of rebound MUA that resembled the adult k complex were also evoked.

(B) K complex could be evoked by cross-modal stimulations (here hand clap).

(C) Population averages for MUA and time spectrogram. Averages are proportion of peak spike rate or power for each animal (dotted line = SD). Older awake animals showed no significant MUA or spectral power elevation following the VEP. During deep sleep, a second peak in MUA caused by the k complex was observed 500–1000 ms after stimulation. Unlike younger animals, however, this evoked burst was not associated with a consistent L4 field potential oscillation.

The Shift from Bursting to Acuity Occurs as a Rapid Switch

To determine the exact timing of the change from bursting to acuity, we analyzed the response characteristics of acutely recorded animals as a function of age. The distribution of evoked MUA duration was bimodal, with the transition between populations occurring between P11 and P12 (Figure 3A). Between P8 and P11 24 of 24 rats had light responses longer than 600 ms (average 1042 ± 249 ms). On P12 the response shortened and was less than 350 ms in 27 out of 28 rats between P12 and P19 (average 219 ± 79 ms; t test $p < 0.00001$). A measure of field potential oscillation, the median number of beta oscillation troughs in the 2 s following stimulation (Figure 3B), showed a similar pattern, though the change occurred more gradually between P11 and P13. In contrast, the delay of the visually evoked response did not show a sharp change but decreased progressively between P8 and P20 (Figure 3C), reflecting primarily retinal maturation (see below). Pigmented Long-Evans rats developed similarly (Figure 3, thick circles).

To examine the developmental sequence in individual rats, we performed chronic recordings from single pups, sampling every 12 hr between P11 and P13 (Figures 3D and 3E). All rats examined (n = 5) largely transitioned from light-evoked bursting to the more mature pattern in under 12 hr. Four switched during the night of P11 and one on P12. Thus, both population analysis of acute recordings and chronic recordings from individual animals suggest that the transition between the bursting and acuity periods occurs as a rapid switch between P11and P12.

The Switch from Bursting to Acuity Is Associated with an Increase in the Amount and Continuity of Spontaneous Cortical Activity

Our chronic recordings revealed a close relationship between ongoing activity and the switch in visual response. Beginning

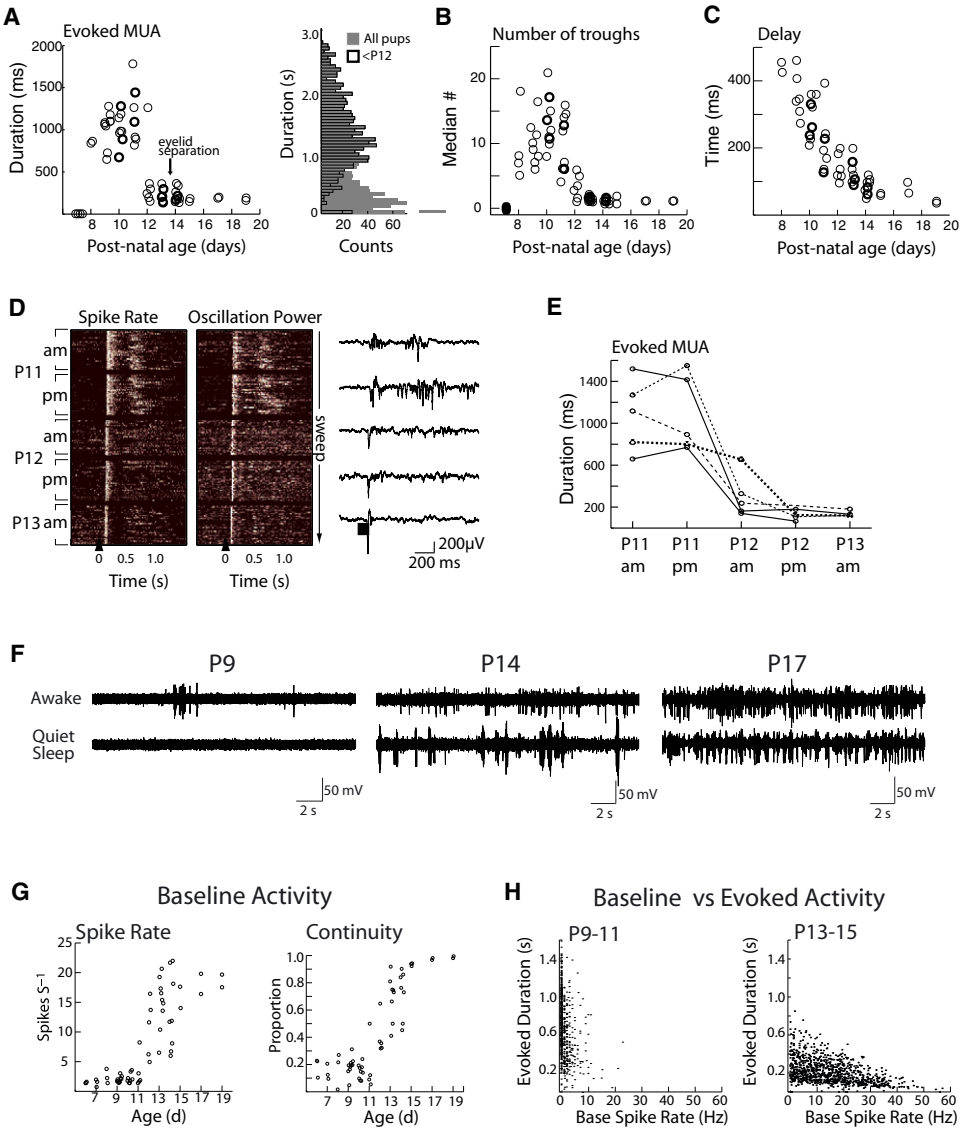

Figure 3. Rapid Switch in Evoked and Spontaneous Activity before Eye Opening in the Rat

(A) Scatter plot of the duration of the evoked response versus age for each pup. Duration was quantified as the amount of time that the spike-rate (50 ms bins) was elevated above baseline. A sharp change in response is observed on P12. Wistar rats = thin circles, Long-Evans = think circles. At right is a histogram of response duration for all trials for all animals. The total distribution is shown by the gray bars and is bimodal, suggesting two populations of response. Overlaid on the gray bars, the black sided boxes show only the events of young pups. Thus, P8–11 animals account for all events longer than 1 s. This bimodal distribution of duration further supports a switch, rather than a gradual reduction, in response duration.

(B) Median number of negative field potential deflections ("troughs," negative peaks greater than 50 μV measured on 5–30 Hz filtered trace) during the 2 s following the stimulation versus age.

(C) Delay to onset of the evoked potential versus age for each animal. Note that delay decreases monotonically with age.

(D) Repetitive recording from a single animal shows that the switch in visual response occurs in under 12 hr. Raster plots show spike-rate (left) and oscillation power (right, summed 5–20 Hz) in 50 sequential trials for five sessions each spaced by 12 hr. An example trace from each recording (2 Hz high pass) is shown to the right. Between the night of P11 and the morning of P12 the response switches from a long-duration oscillatory event to a singular VEP.

(E) Duration of MUA response for five pups recorded sequentially as in (D). Four out of five experienced the switch on the night of P11, while one did so during the day of P12.

(F–H) Switch in visual response is associated with an increase in the amount and continuity of spontaneous cortical activity. (F) Spontaneous MUA activity in L4 of V1 recorded in the dark during different arousal states in the same P9 (left), P14 (middle), or P17 (right) animal. (G) Scatter plots of pre-trial MUA versus age (left) and continuity of MUA versus age. An increase in both rate and continuity was observed between P12 and P15, following a period of low activity first to second postnatal weeks. (H) Scatter plots of spike rates during the pretrial period (500 ms) versus the duration of the evoked response for that trial. Response duration was negatively correlated with spontaneous activity rate at both ages.

See Figure S2.

at the end of the second week, we observed an increase in spontaneous MUA, both in the frequency of isolated spikes when the pups were awake, as well as in the occurrence of bursts during quiet sleep (Figure 3F). Quantification of the spontaneous spike rate as well as the continuity of spiking (as the proportion of 500 ms bins with at least one spike) showed that both basal spike rate and continuity remained low between P6 and P11, becoming more continuous and frequent on P12 (Figure 3G). These parameters then further increased steadily over the third postnatal week. To test if the increase in spontaneous activity is causally related to the loss of bursting responses, we correlated spike rate during the pretrial period (500 ms) to the duration of the evoked MUA response for each individual stimulation (Figure 3H). Within both age ranges, there was a significant negative correlation between spontaneous spike rate and the visual response (P9–11: $r = -0.31$, $p = 0.0001$; P13–15: $r = -0.31$, $p < 0.0001$). In particular, while short duration responses were observed at all spontaneous spike rates, long duration responses only occurred following quiet periods. Thus a simple increase in spontaneous baseline activity will substantially reduce, if not nearly eliminate, long-duration responses.

We examined the role of early visual experience in early visual development by dark-rearing or forced eye opening at from P7. Neither manipulation affected the timing of the switch (Figure S2).

In Humans the Switch in Light Response Occurs Prematurely

Using the parameters developed in the rodent, we examined neocortical activity in human preterm infants using electroencephalography (EEG) to see if they have a similar bursting period of visual processing. Preterm human infants born at 25 to 36 weeks of gestational age (GW) were examined between GW27and GW42 (term is GW37–40) using the standard clinical nine electrode arrangement (Figure 4A). High-pass filtering characteristics (>0.05 Hz) and stimulation intervals (at least 10 s) were kept similar to those used for the rodent. Stimulation was given during periods of quiet sleep. We did not record from infants young enough to observe a light *Blind* period but did clearly observe two distinct periods of *bursting* and *acuity* that resembled those found in the rats.

In eight of nine human infants examined between GW27 and GW34, 100 ms light flashes evoked detectable visual responses at occipital electrodes (see Figure S3; Movie S1). This response consisted of two large amplitude, slow, negative deflections that were most prominent on the occipital electrodes (Figure 4B). The second, larger deflection contained rapid oscillations (5–20 Hz; Figure 4C) and resembled spontaneously occurring delta brushes (Dreyfus-Brisac and Monod, 1965). After GA36 weeks (GW36–42), light flashes no longer evoked the large amplitude slow waves, nor the fast oscillations seen in younger infants. Instead, light flashes evoked smaller negative deflections characteristic of the VEP in term infants (Figure 4C). In contrast to the large immature response, the VEP was small relative to baseline activity and thus variable between infants, another characteristic of these ages (Kraemer et al., 1999; Ellingson, 1970).

We quantified the duration of the rapid oscillations, the peak amplitude of the evoked potential, and the delay to the initial response for each infant (Figures 4D–4E). Duration and amplitude evidenced a bimodal pattern, with the switch occurring between GW34 and GW36, 1 to 3 weeks before normal term. Like in the rodent, light-evoked responses in the younger infants were longer and larger. Also similar to the rodent, the development of delay was more regular, without evidence of bimodal distribution. Post-stimulus time course averages were calculated for infants before and after the switch. During the bursting period, the initial response and evoked delta brushes occurred with a delay to peak of 312 ± 21 ms and 818 ± 35 ms, respectively ($n = 8$ neonates; Figure 4F). The first peak is consistent with the location of the large negative potential described in previous studies, termed N2 (Pike et al., 1999). The second negative wave, as a result of the evoked delta-brush, was longer and larger than the initial response and contained a prominent beta-band oscillation (Figure 4F, bottom). We used the fact that the infants typically lay with one eye partially obscured to examine the localization of visual responses (Figure 4G). Both the initial response and evoked slow component of the delta-brush were more localized to occipital electrodes, though no lateralization of the response was observed. At the older ages, the first negative potential (peaking around 240 ms) was predominantly observed at contralateral occipital and temporal electrodes, while the later slow components were distributed among both occipital electrodes.

The time period between GW34 and GW36 is recognized as an important transitional point in the development of the EEG; from this age infants show clear EEG distinction of sleep states (as judged by percent of time in indeterminate sleep) and exhibit longer periods of continuous polyfrequency EEG activity during active sleep and wakefulness and shorter silent periods during quiet sleep (André et al., 2010). To understand if these changes resulted in increased baseline activity similar to that observed in the rats, we examined the amount of pretrial activity at occipital electrodes by measuring the standard deviation of the EEG signal for each infant. As expected we observed an increase in spontaneous EEG activity between GW34 and GW36 (Figure 4H) in line with the time of the switch.

Thus, in both humans and rodents the first visual response is a complex of very large amplitude potentials and rapid oscillations that resemble spontaneously occurring activity. In both species the switch to "mature"-like evoked responses consists of a reduction in the duration and amplitude of the visual responses, that occurs just before the onset of patterned vision in synch with an increase in continuous baseline activity.

Changes in Intracolumnar Processing between Bursting and Acuity Periods

The functional and mechanistic bases of these conserved changes in visual response were further examined in rats. Changes in intracortical processing were determined by observing the flow of the visual response through the cortical column using 16-site linear electrode arrays (Supplemental Experimental Procedures). The mature VEP has a characteristic columnar flow, with a prominent sink in L4 that spreads to L2/3 (Mitzdorf, 1985). During the bursting period however, the initial response consisted of an early and repetitive potential (the gamma burst) restricted to and driving MUA specifically in L4,

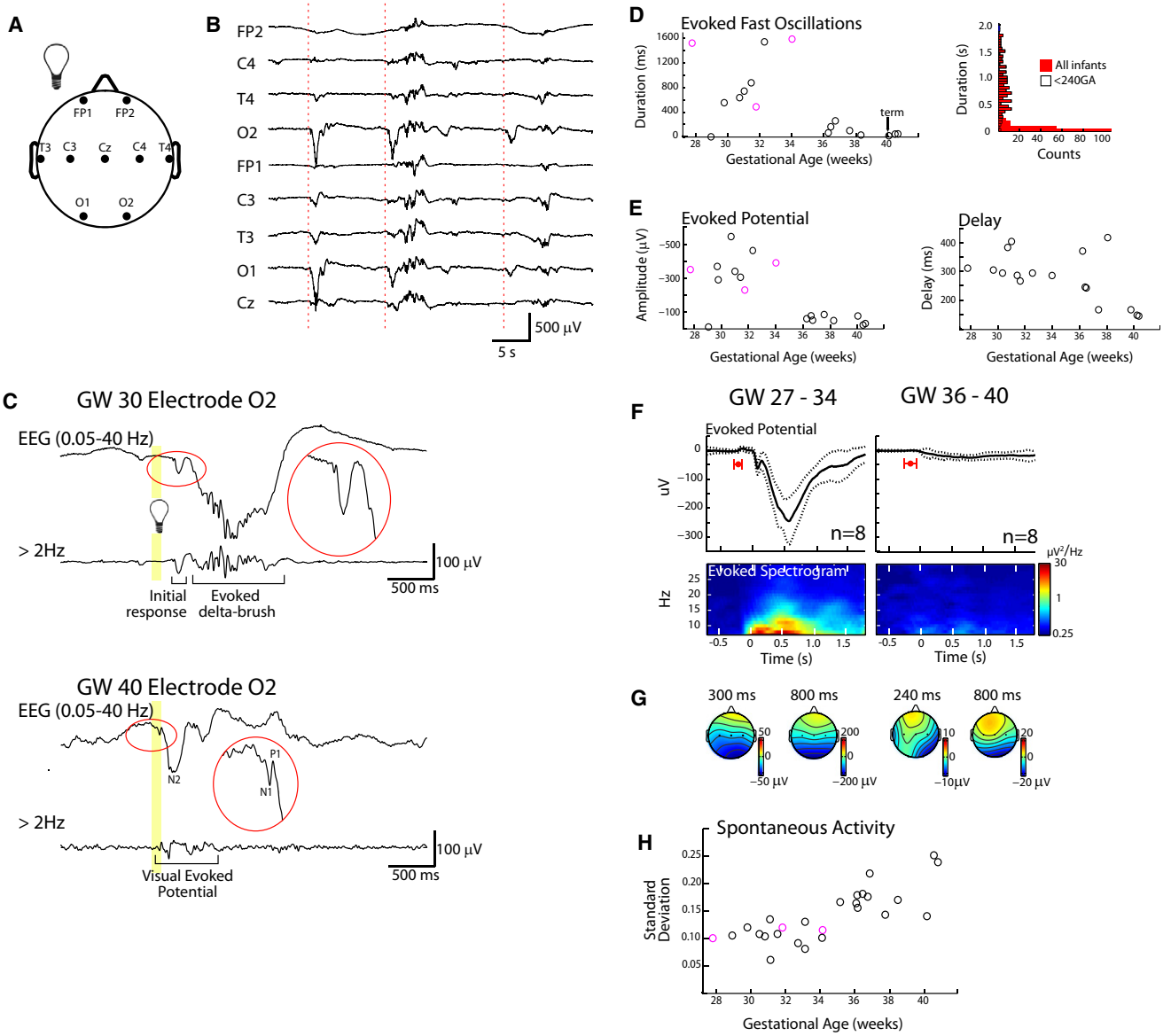

Figure 4. Bursting and Acuity Periods in Preterm Human Visual Development

(A) Electrode placements for EEG recordings of neonates (modified 10–20 international placement).

(B) EEG traces from all electrodes (relative to ground, negative down) during quiet sleep in an infant during the thirtieth gestational week (GW). Whole-field 100 ms light flashes were applied at the red lines and evoked high-voltage slow waves at occipital electrodes. More diffuse activity sometimes occurred spontaneously (or at a longer latency to stimulation) on other electrodes.

(C) Representative occipital light response at GW30 and GW40. The younger infant shows the high-amplitude slow waves and rapid oscillations (delta brush) similar to rats; the older infant's response is smaller in amplitude and duration and has some of the grapho-elements typical of the flash-evoked VEP. For each infant the top trace shows all frequencies between 0.5 and 40 Hz; the bottom trace has been high-pass filtered above 2 Hz to show the fast oscillations that occur within the larger, slower wave. The initial response is enlarged in the red circle. Identifiable elements of the visual evoked potential are marked for the term infant.

(D) Duration of the evoked fast oscillations versus age for each infant (left). Duration was quantified as the amount of time the summed power between 5 and 20 Hz (100 ms bins) was statistically elevated over baseline. A loss of the long-duration fast oscillations occurred between GW34 and GW36. A single infant recorded on multiple days is represented in red. A histogram of response duration for all trials in all infants as described for Figure 3A is presented at right.

(E) Peak amplitude of the evoked potential (left) and delay (right) versus age for each infant.

(F) Population averages of the light-evoked potential (dotted line = SD) at the occipital electrode contralateral to the light flash. Below is the average time-series spectrogram of the same population to show the fast-oscillatory responses. Responses were aligned to the beginning of the negative deflection (0 s) and the mean ± SD time of flash is shown in red.

(G) Population average response maps for each age group showing the localization of evoked potentials during the initial response (at 300 or 240 ms delay) and of the long delay response (800 ms).

likely indicating a thalamic origin (Figure 5A, left). This gamma burst was curtailed by a sharp wave that included firing in all cortical layers. This "columnar burst" was analyzed by determining the average field potential and MUA in all layers aligned to peak of spiking activity in L6 (n = 11 P9–11; n = 9 P13–14). This showed activation of all cortical layers following a buildup of L4 firing (Figure 5B) and current sinks at the border of L3 and L4 and in L5/6, with prominent sources at the surface and below L4. In contrast, by P13 the VEP acquired an adult-like pattern, with a single current sink that started in L4 and traveled up to L2/3. It lost the prominent deeper sink and its associated surface source (Figure 5A, right, and Figure 5B, bottom). The spiking response also changed, becoming shorter, and more heterogeneous between layers, as units in upper L5 ceased to be strongly activated by the stimulus.

We further examined the precision of the second-order spiking response by cross-correlation analysis of L2/3 spike rate with the spike rates in the other cortical layers (Figure 5C). As expected, in P9–11 rats superficial MUA was correlated with zero time lag to L5 and L6 MUA, consistent with their firing as a unified burst. The cross-correlation showed a slight lag to L4, consistent with them following on the summation of these inputs. At P13–14 L2/3 units were correlated with a slight lag to units in L4 but poorly to L5/6, consistent with a direct drive by the input layer following the switch. Thus, our interlaminar analysis confirmed the hypothesis that second-order layers switched from being driven by a multilayer burst, to a specific drive by L4. Therefore, in addition to the disappearance of delta brushes, the developmental switch in visual processing from *bursting* to *acuity* results in the assumption of intracolumnar visual processing similar to the mature pattern.

The large-scale columnar bursting observed in younger animals has a laminar profile similar to that observed in adult visual cortex during bursting mode (Swadlow et al., 2002), suggesting a similar detection function for the primitive visual response (Sherman and Guillery, 2009). We tested this hypothesis by measuring L4 MUA during the initial response to varying luminance (Figure 5D). Four of four pups recorded during the bursting period showed a sharp transition between no response and maximal response. During the acuity period, however, 4/4 pups had a graded response to varying luminance. The 95% confidence intervals for the widths of sigmoid curves fitted to the responses of each pup did not overlap for any young compared to old pup (Wilcoxon rank-sum median difference, p = 0.02). The inflection points were not different between groups, however. Thus, before the switch, visual responses work as a burst mode with even minimal stimulation resulting in large all-or-none cortical responses.

We further examined the development of visual processing by determining response depression to 1, 3, and 10 Hz (10 s) presentations of 30 ms flashes (Figure S4). In five of five P10–11 pups examined, field potential and MUA responses displayed complete depression at all frequencies. In stark contrast however, five of five P13–14 pups could follow frequencies at high as 10 Hz, though the responses depressed in a frequency-dependent manner.

In total, our results suggest a rapid and simultaneous acquisition of many of the key components of mature visual processing just before eye opening.

Cortical and Retinal Contributions to the Switch

The switch in visual response from bursting to acuity involves a change of the gamma oscillations to a singular potential as well as the loss of columnar bursts and delta brushes. To dissociate retinal and thalamocortical contributions to these changes, we examined the responses evoked in visual cortex by direct electrical stimulation of the optic nerve (Figure 6). To avoid the generation of retinal waves, we injected glutamate receptor antagonists CNQX (500 μM) and AP5 (2.5mM) intraocularly. In all rats before the switch (P9–10, n = 3) electrical stimulation evoked a singular negative sharp wave with short latency, that resembled the VEP after the switch. However, electrical stimulation still evoked delta brushes and columnar bursts indicating a thalamic or cortical locus of their generation. After the switch (P13–15, n = 5) electrical and light stimulation strongly resembled one another. Both had VEPs but no delta brushes or columnar bursts (Figure S5A). These electrical stimulation experiments allowed measurement of the relative roles of retinal and thalamocortical processing in determining the response delay. In P9–10 pups, visual responses occurred with a delay of 200 ± 10 ms, whereas electrical stimuli evoked a response at a delay of 36 ± 1 ms. At P13–14 the decrease was from 59 ± 5 ms to 17 ± 2 ms. Thus, a large majority of the developmental reduction in delay is due to changes in the processing speed of the retina.

Retinal responses were directly investigated in excised retinas of P10–17 pups (Figures S5B and S5C). We observed a rapid acquisition of a short-latency, coherent light response on P12–13. However, all retinas between P10 and P15 exhibited a similar long-duration elevation of ganglion cell firing. These results suggest that the development of a singular VEP largely involves retinal maturation, whereas the developmental elimination of deep bursts and delta brushes involves changes in thalamus or cortex.

Dependence on Ascending Neuromodulators

The close temporal association of the switch from bursting to acuity modes with a strong modulation of cortical activity by vigilance state suggests a role for the ascending neuromodulatory systems. As a first test of this hypothesis, we examined light responses in P13–15 pups following acute surgical isolation of the cortex from mid and hind brain structures (*cerveau isolé* [CI]). Compared to control surgery or hind-brain only disconnection, lesion at the midcollicular level reduced the continuity of ongoing activity and reinstated light-evoked delta brushes (Figure 7; Table S1). CI did not modify the initial response. To examine the role of cortex in mediating this neuromdulatory response we applied norephinephrine (NE, 100 μM) directly to

(H) Baseline activity versus age. Activity is measured as SD as proportion of peak amplitude for each infant. As in rats, the loss of light-evoked high-voltage bursts was accompanied by an increase in spontaneous cortical activity. Five additional infants not assayed for light responses were included in this analysis. See Figure S3 and Movie S1.

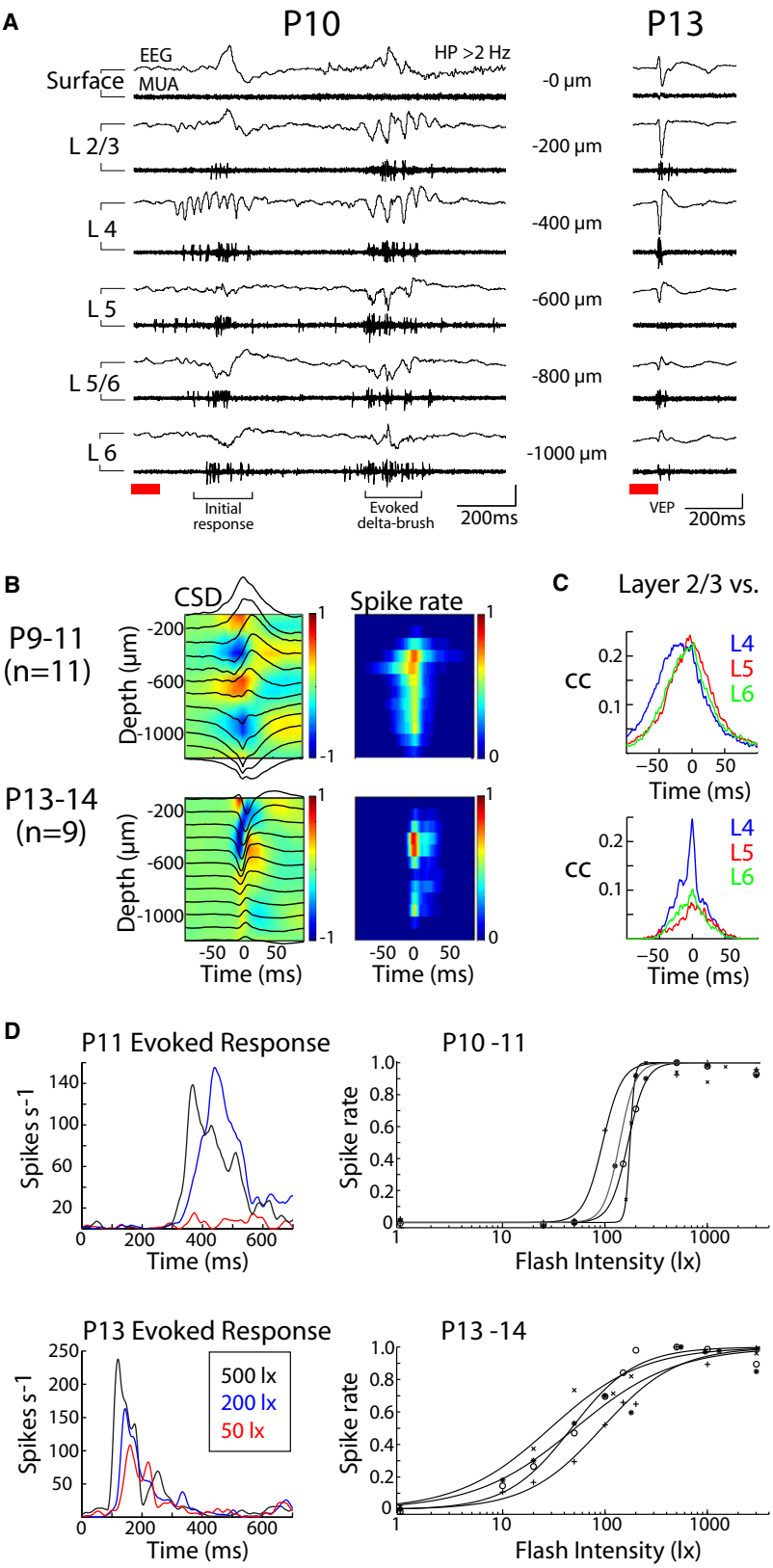

Figure 5. Developmental Elimination of Light-Evoked Bursting Is Correlated to Maturation of Intracolumnar Processing and Graded Visual Responses in the Rat

(A) Multielectrode linear-array recordings show changing intra-laminar circuitry. P10 (left) and P13 (right) example traces show field-potential (scale bar = 200 µV) and MUA activity (scale bar = 50 µV) at multiple cortical depths. At P10 the gamma-burst oscillations of the initial response were limited to L4. Engagement of other layers came as a burst that spread throughout the column. The second event (evoked delta-brush) involved more robust, rhythmic activation of all layers. At P13 only a single mature VEP with no delta-brush remained. The VEP started in input layers and spread to superficial ones. Unit firing occurred as discrete bursts closely associated with the negative potential.

(B) The average current source density (CSD; left) and spike-rate (right) for each period using L6 spike-rate triggering during the initial response.

(C) L2/3 spike cross-correlation analysis made during the initial burst showed that the superficial layers were broadly correlated with all other layers during the bursting period but specifically followed L4 after.

(D) Graded visual responses emerge after switch. Post-stimulus time histograms of spike rates in L4 during the initial response (right) show nongraded all-or-none bursting to various stimulation intensities in a P11 pup, but graded responses in a P13 pup. Sigmoidal curves fit to the intensity responses for four rats in each age group (left) show that the dynamic range of young pups is much smaller than after the switch.

See Figure S4.

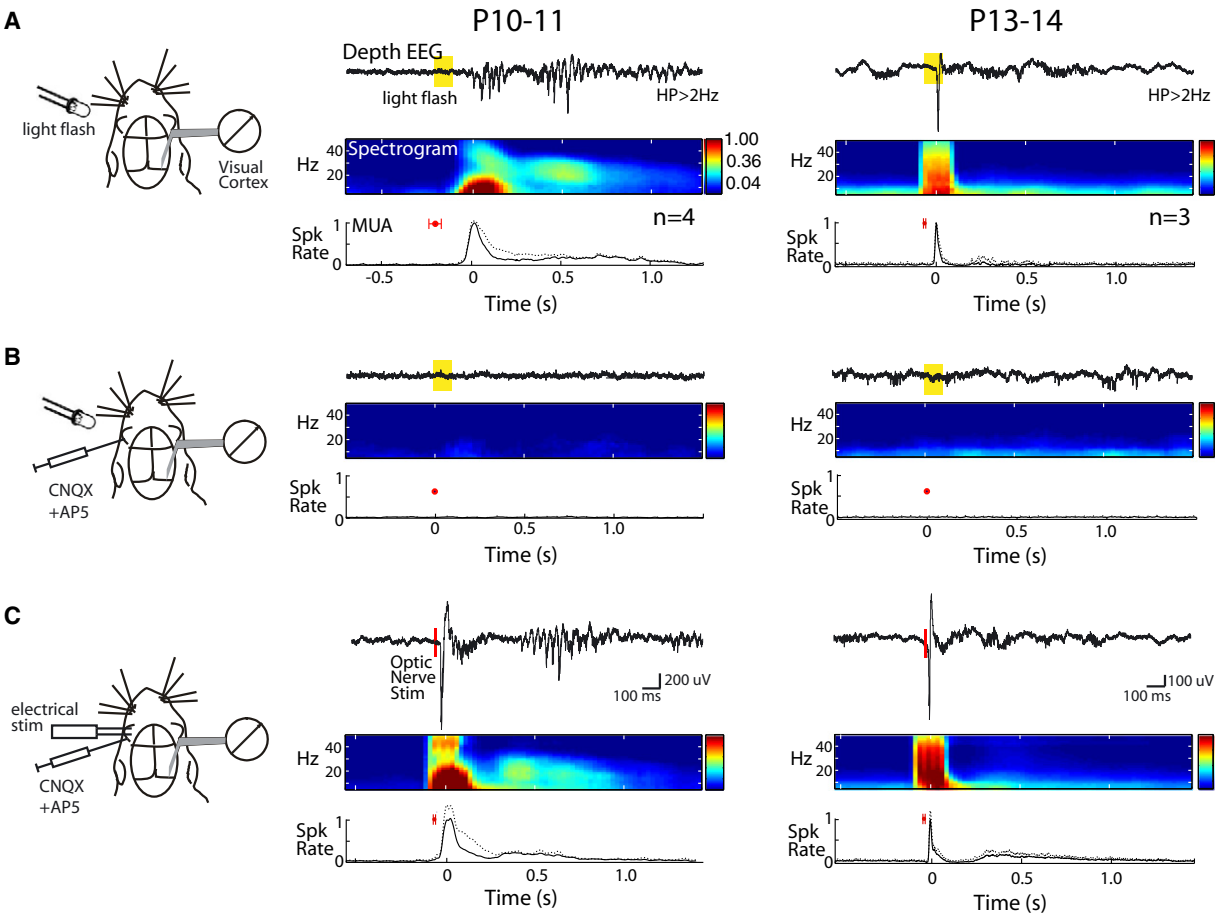

Figure 6. Thalamocortical Networks Determine Early Bursting

(A) Flash-evoked response in V1 during bursting (left) and acuity (right) periods in the rat. Example traces (P10 and P13, respectively) are shown above the population average time-series spectrogram and the average MUA time course (dotted line = SD).

(B) While recording from the same cortical position, retinal circuitry was disrupted by intraocular injection of glutamate receptor antagonists. Blockade was verified by assaying absence of a light-response.

(C) Direct electrical stimulation of the optic nerve (1 ms) while blocking retinal activity produced a single sharp potential with short delay similar to the acuity VEP but still evoked columnar bursts (Figure S5) and delta-brushes at longer latency. After the bursting to acuity switch, both light and optic nerve stimulation evoked a sharp VEP but not delta brushes.

See Figure S5.

the cortical surface of CI pups (n = 5). This application desynchronized ongoing activity (increasing continuity but not baseline spike rate) and eliminated evoked delta brushes. The effects of CI could be mimicked by subanesthetic doses of urethane (0.5 g/kg i.p.; Figure 7; Table S1), showing that it is regulation of vigilance state, not nonspecific surgical damage, which drives the reinstatement of delta brushes.

Inhibition of Immature Bursting by $GABA_A$ Receptor Currents

Maturation of GABAergic inhibition determines many developmental changes in cortical activity and plasticity (Daw et al., 2007; Huang et al., 1999; Long et al., 2005). The developmental expression of KCC2, a chloride channel that determines Cl^- driving force, is correlated with the developmental elimination of human delta brushes (Vanhatalo et al., 2005). However, delta brushes are spatially and temporally limited by $GABA_A$ receptor signaling in barrel cortex (Minlebaev et al., 2007). To test the involvement of the maturation of $GABA_A$ receptor signaling in the visual response, we increased $GABA_A$ currents with diazepam, a positive allosteric modulator, or inhibited $GABA_A$ currents with bicuculline (Figures 8 and S6). Local cortical surface administration of diazepam (1.6 mM; n = 4) during the bursting period had an inhibitory effect on the visual response, reducing the post-stimulus spike rate (1 s, 51% ± 14% [mean ± SEM] of control, p = 0.03 difference from 100 by sign-rank test) and suppressing the rapid delta brush oscillations (22% ± 7% of control [20–25 Hz]), p < 0.001). In place of evoked delta brushes, we observed disorganized bursting with a peak frequency between 5 and 10 Hz. Systemic injection (2 mg/kg; n = 5) had no further effect on these parameters. Systemic diazepam did affect the initial response, however. Cortical

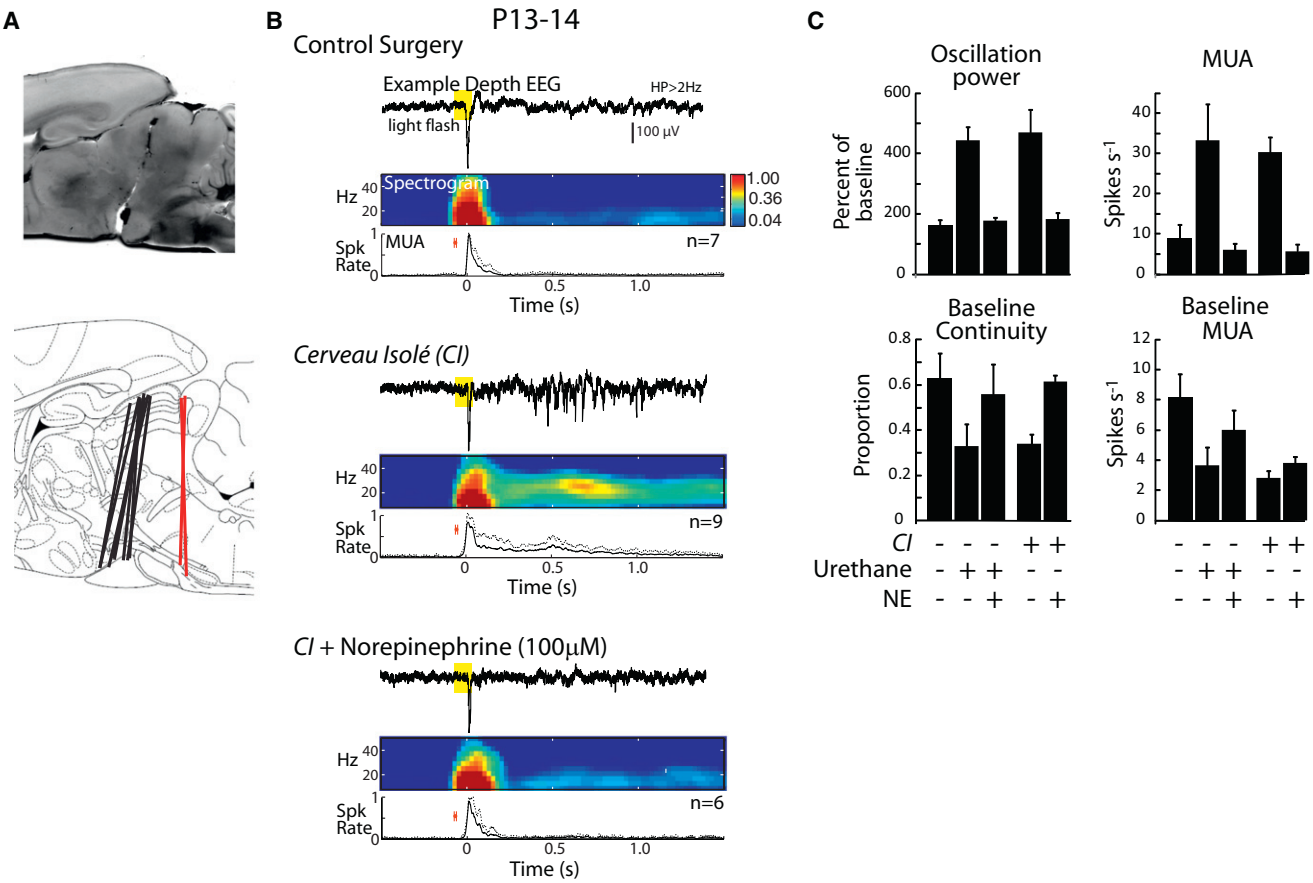

Figure 7. Role of Ascending Neuromodulators in Mediating the Switch

(A) Isolation of forebrain via a midcollicular cut (*cerveau isolé* or *CI*) during the acuity period was used to examine the role of the ascending activating systems in maintaining the continuity of spontaneous cortical activity and acuity response in the rat. Location of cuts determined post-mortem is shown on a schematic drawing (black lines), while two more posterior cuts that did not affect activity are shown in red.

(B) Flash-evoked response in V1. An example trace (P14 pup) is shown above the population average (P13–14) time-series spectrogram and the average MUA time course for three conditions: (top) control littermates that received needle insertion without cut, (middle) CI and (bottom) CI with norepinephrine (NE) added to the cortical surface. CI did not affect the VEP but restored oscillatory after-discharges which were then eliminated by NE.

(C) Quantification of CI and urethane treatment. Oscillation power (increase in 20–30 Hz over baseline) and MUA 300–1500 ms after stimulus (time of evoked delta brushes) was used to quantify treatment effects (top graphs). In addition to CI experiments, urethane (0.5 g/kg i.p.) was given to control pups (n = 6) followed by surface application of NE (n = 5). Ongoing activity (bottom graphs) was measured as in Figure 3G. Urethane and CI both reduced continuous ongoing activity and reinstated oscillatory after-discharges, and NE suppressed these effects. Error bars in (C) are SEM.

application did not affect gamma oscillations, though the total amplitude of the slow wave was reduced (Figure 8D). Systemic administration, by contrast, eliminated the gamma oscillations, leaving only a single negative potential that resembled the mature VEP in shape, though not amplitude. Systemic diazepam had comparably little effect on the P13–14 visual response (Figure S6). Thus, increases in GABAergic synaptic effectiveness in retina or thalamus may contribute to the development of the VEP. However a change in $GABA_A$ currents from excitatory to inhibitory is unlikely to play a role in the switch.

We further examined this hypothesis by systemic injection of the NKCC1 blocker bumetanide (5 μmol/kg), which shifts the GABA driving force to hyperpolarizing in vitro (Tyzio et al., 2006; Yamada et al., 2004) and blocks hippocampal giant depolarizing potentials in vitro and sharp waves in vivo (Dzhala et al., 2005; Sipilä et al., 2006). Bumetanide had no effect on visual responses at P9–11 (n = 3). Furthermore, epipial application of bicuculline (50 μM) at P10–11 had an excitatory effect, increasing the amplitude of the columnar burst (Figure S6). The frequency of the rapid oscillations during delta brushes was not affected however, showing that while increasing cortical GABA inhibition can suppress delta brushes, it is not necessary for the pacing of the rapid rhythms.

The Timing, but Not Occurrence, of the Switch Is Sensory Modality Specific

We next examined spontaneous and evoked activity in the barrel cortex, where whisker stimulation evokes delta brushes during the first postnatal week (Minlebaev et al., 2007, 2009) yet patterned somatosensory perception (in the form of whisking) is initiated 2–4 days before eye opening (Landers and Philip Zeigler, 2006). In line with the hypothesis that the loss of sensory

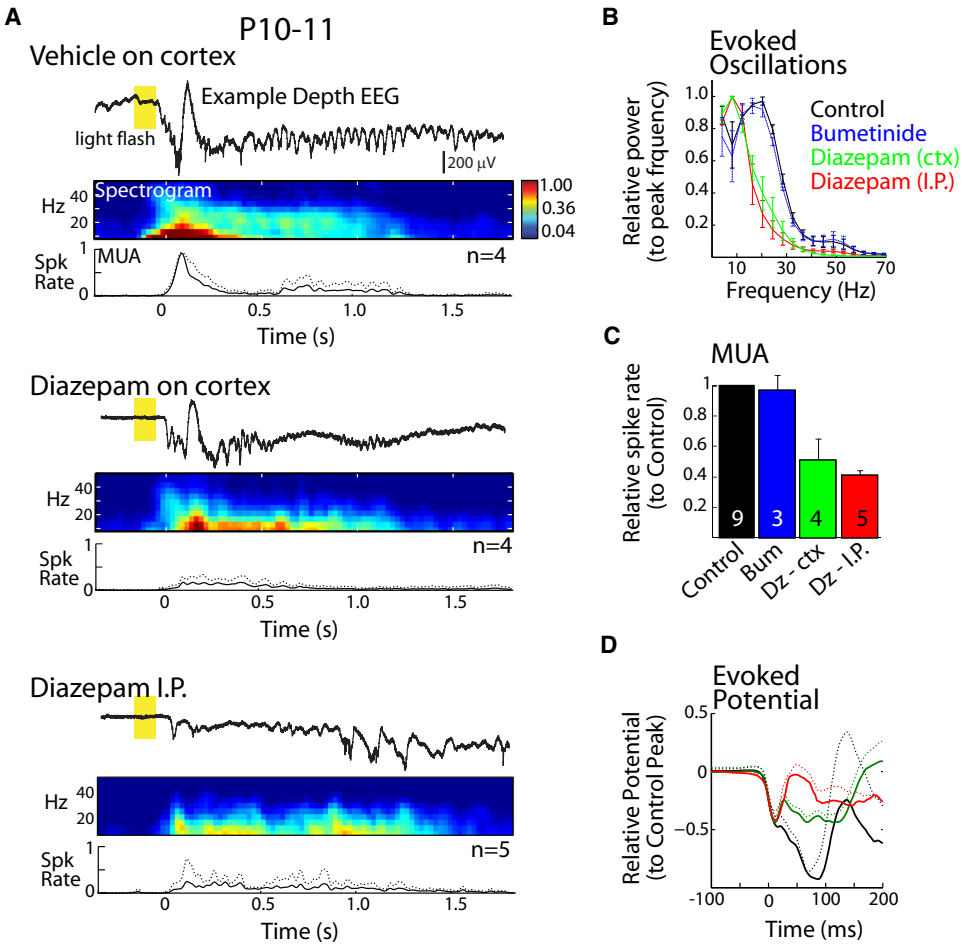

Figure 8. Inhibitory GABA in Cortical Circuits before the Switch

(A) An example trace is shown above the population average time-series spectrogram and MUA time-course for three conditions: control recordings, diazepam on cortical surface, and diazepam i.p. The example traces are from the same P10 pup. MUA and power are relative to peak control activity.

(B) Frequency distribution (5–70 Hz) of evoked long-latency (300–1500 ms) activity. Cortical diazepam eliminated evoked rapid oscillations but allowed disorganized 8–12 Hz activity. Bumetanide, which shifts $GABA_A$ synaptic currents from excitatory to inhibitory in immature neurons in vivo, had no effects on visual responses.

(C) Post-stimulus MUA (0–1500 ms).

(D) Mean evoked potentials (wide-band depth EEG, n = 3) show a differential effect of cortical and systemic diazepam. Cortical diazepam reduced the amplitude of the evoked potential but did not prevent the gamma oscillations (see also A, middle graphs), while i.p. injection eliminated these oscillations which were replaced by a single potential.

(B) and (C) error bars are SEM. See Figure S6.

evoked bursting is timed to precede mature sensory inputs, we observed a similar loss of evoked air puff evoked delta brushes between P8 and P9, earlier than in the visual system (Figure 9). Like visual cortex, the switch in barrel cortex responses was correlated with an increase in spontaneous activity. Thus, the timing of the loss of immature bursting is sensory system specific and coincides with the emergence of continuous activity and shortly thereafter, the onset of high-frequency sensory input.

DISCUSSION

We have used light as a probe to study thalamocortical network properties during early development in preterm humans and neonatal rodents. We identified two distinct modes of cortical function (Figure 10A), a "bursting" mode characterized by long periods of network silence during which weak retinal output is amplified by large and long-lasting cortical oscillations (Figure 10B) and an adult-like "acuity" mode beginning just before birth in humans and eye opening in rats. The acuity mode was characterized by an increase in the continuity of ongoing cortical activity, the emergence of clear vigilance state differentiation and visual responses with a number of features consistent with the acquisition of a minimal capacity for image processing, including graded, sharp responses capable of sustained activity. The transition from bursting to acuity occurred as a rapid switch (several hours in the rat) timed not to eye

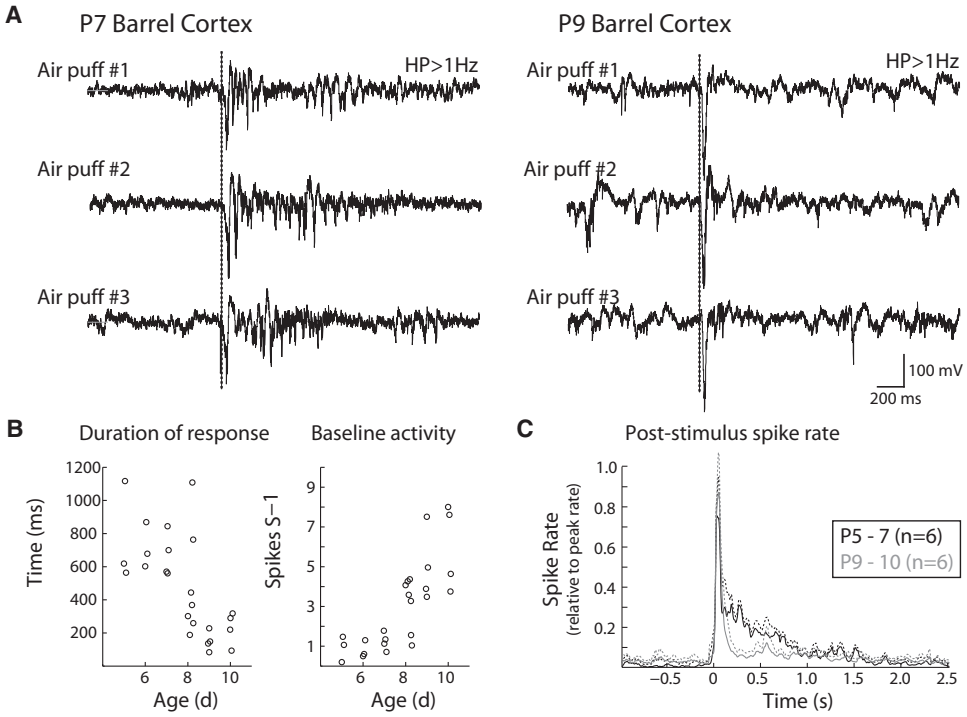

Figure 9. Rat Somatosensory Responses Switch from Bursting to Acuity Earlier

(A) Evoked somatosensory responses were assayed in barrel cortex via air puffs applied to the whiskers. Three representative whisker responses show evoked oscillations to whisker stimulation at P7 (left) and their loss by P9 (right). Air puffs generated a sharp evoked potential at both ages.

(B) Rapid loss of long-duration evoked activity by P9 was correlated with an increase in spontaneous activity. Scatter plots show the duration of evoked MUA (left) and spontaneous spike rate (right) versus age for each hemisphere from 14 rats. Both parameters showed sharp changes similar to the visual system, but 3–4 days earlier.

(C) Population average post-stimulus MUA from before (black) and after (gray) the switch. Rate was calculated for a 20 ms sliding window (dotted line = SEM).

opening per se, but specifically to a behaviorally relevant parameter, the onset of patterned vision. Activity in barrel cortex underwent a similar transformation timed to the initiation of whisking, indicating it is a general feature of sensory cortex development, the timing of which is modality specific. Remarkably, despite synaptic plasticity following eye opening (Lu and Constantine-Paton, 2004; Quinlan et al., 1999), the switch was independent of visual experience but still involved coordinated changes at multiple levels in the visual system, notably the strengthening of retinal responses, an increase in functional inhibition, and a change in thalamocortical networks that depends on ascending neuromodulators (Figure 10C).

Altogether our results demonstrate a singular cortical state present during early development that is specialized for the transmission and amplification of weak and infrequent peripheral activity such as spontaneous retinal waves. This primitive response mode influences sensory responses and thus is actively downregulated by the development of cortical vigilance states in order to facilitate sensory processing.

Initiation of a Continuous Mode of Cortical Activity Ends the Bursting Period

Several lines of evidence implicate the emergence of a continuous (aka activated or desynchronized [Steriade and McCarley, 2005]) mode of thalamocortical function as central to the switch from bursting to acuity. First, the timing of the switch is tightly correlated with a sharp increase in the amount and continuity of spontaneous activity in rat visual and somatosensory cortex and in the occipital poles of humans, and this increase directly suppressed bursting in individual trials. The correlated increase in continuous activity and elimination of spontaneous delta brushes, a transition that occurs, like in the rat, initially in central, and lastly in occipital regions, is well described in preterm infants (Tolonen et al., 2007; André et al., 2010). Second, isolating the forebrain from ascending neuromodulatory arousal inputs reverted spontaneous cortical activity and visual responsiveness to the immature mode of discontinuity and bursting, respectively. Both parameters were reinstated by cortical application of norepinephrine, a key initiator of the activated cortical state (Berridge and Waterhouse, 2003; Foote and Morrison, 1987).

Studies in adults show that periods of neuronal silence during slow wave sleep or quiet wakefulness encourage the generation of thalamic bursting (Sherman and Guillery, 2009), columnar activation (Swadlow et al., 2002), and down-up state transitions (Hasenstaub et al., 2007; Petersen et al., 2003; Sachdev et al., 2004). Thus, the much longer down states and apparent lack of effective activation by neuromodulators during the bursting period should massively increase the probability sensory

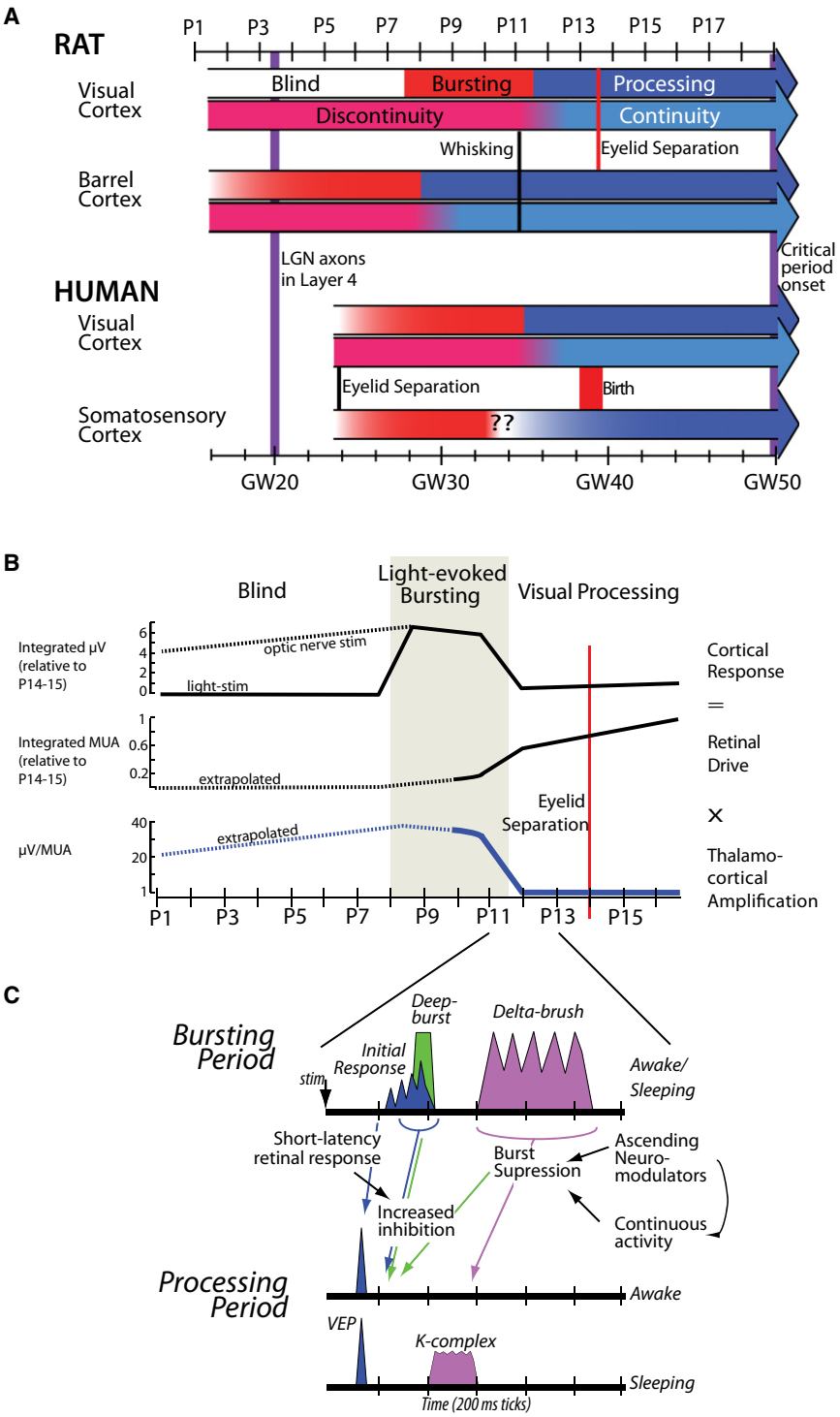

Figure 10. Early Development of Sensory Processing in Humans and Rats

(A) Developmental templates of sensory development. Timelines are aligned to independent time points: the arrival time of LGN axons (P3.5 rat, 21GW human [Finlay and Darlington, 1995]) and the onset of monocular deprivation plasticity (8–10 weeks human [Birch and Stager, 1996], P19 rats [Fagiolini et al., 1994]). The timing of the switch in human somatosensory cortex is not known, although delta brushes were evoked in GW33 infants (Milh et al., 2007). In humans, the switch in somatosensory and visual regions is more closely aligned with birth, while the switch timing is independently regulated in rat.

(B) Hypothesized relationship between retinal and cortical activity during early visual development. The integrated voltage deflection in V1 (solid line top trace; from Figure 1G) and the integrated retinal MUA (middle trace; from Figure S5) following light stimulation are shown relative to the response after eye opening. During the first postnatal week, light stimulation does not cause a cortical response. However, electrical stimulation can trigger bursting (top trace dotted line; Hanganu et al., 2006). Dividing the cortical response by retinal output shows clear thalamocortical amplification during the bursting period.

(C) Summary of identified factors contributing to the switch in sensory processing. Each of the three component parts of the immature response and their hypothesized adult homolog is color coded. The direct mechanism leading to their transformation is shown breaking the color coded line, while factors modulating these factors are shown as black arrows. For example, the gamma-burst transforms into the VEP as a result of short latency response development in the retina and increased inhibition (which may be brought about via the former).

responses will be amplified by recurrent excitation in cortical and thalamocortical networks. The switch is observable in quiet sleep in both humans and rats, indicating that this switch is not simply the development of an awake cortical state but an increase in the relative activation observed during all vigilance states.

While a causal role for the emergence of a continuous mode of cortical activity in the regulation of visual responses seems clear, the question of what underlies the emergence of this activated mode per se remains only partly understood. Certainly the *cerveau isolé* experiments suggest that maturation of the brainstem input to the cortex is an important factor. In fact, the switch coincides with the emergence of clearly differentiable sleep states in both species (Jouvet-Mounier et al., 1970; André et al., 2010), as well as rapid maturation of cholinergic and noradrenergic afferents and receptor distributions (Mechawar and Descarries, 2001; Robertson et al., 1985; Latsari et al., 2002; Venkatesan et al., 1996). However, many aspects of brainstem and forebrain arousal systems operate well before the switch. For example, infant rats and humans show behavioral sleep-wake cycles, state dependent firing of hindbrain sleep

control neurons (Karlsson et al., 2005), and modulation of cortical EEG patterns by sleep state (Seelke and Blumberg, 2010). Furthermore, functional monaminergic and cholinergic connections are in place long before this switch (Hanganu et al., 2007; Johnston and Coyle, 1981).

Thus, the acquisition of brainstem control of cortical states likely requires more than a simple engagement of neuromodulatory systems, but also thalamocortical changes. A prominent candidate is the strengthening of long and short range intracortical connectivity, required for maintenance of the activated cortical state (Sanchez-Vives and McCormick, 2000; Shu et al., 2003). A number of observations are consistent with an increase in functional cortical connectivity over this time period. First, while k complexes and sleep spindles, stimulated by light in adults, are synchronized throughout cortex (Amzica and Steriade, 1998) via horizontal cortical and corticothalamic connections (Contreras et al., 1996, 1997), delta brushes are local events (Khazipov et al., 2004; Yang et al., 2009). Second, in adults, episodes of network silence (''down states'') during sleep do not exceed 500 ms (Steriade and McCarley, 2005), whereas the silent periods in the young rat pups or preterm infants can run to tens of seconds. Such long silent periods are observed in cortical slabs and slices; i.e., under conditions of markedly reduced cortical connectivity (Sanchez-Vives and McCormick, 2000; Steriade and McCarley, 2005; Timofeev et al., 2000). Finally, the network of horizontal connections between pyramidal neurons emerges shortly before eye opening in cats (Callaway and Katz, 1990; Galuske and Singer, 1996) and ferrets (Durack and Katz, 1996; Ruthazer and Stryker, 1996) independently of visual input. In humans, dense horizontal connections are also first observed at GW37 (Burkhalter et al., 1993) and interhemispheric synchrony becomes common in EEG (André et al., 2010). Therefore, we propose that emergence of the continuous mode of cortical activity results from a coincidence of two developmentally regulated factors: (1) maturation of the brainstem arousal input to the cortex, which provides tonic neuronal activation and (2) formation of excitatory synaptic connections between the cortical neurons, which are needed for maintenance of the activated cortical state.

It may seem paradoxical that the emergence of an activated cortical state exhibits regional heterochrony. However, our two factor model can help explain this. Regional variation in the density or pattern of innervation (Foote and Morrison, 1987), and/or in intracortical connectivity (Rakic et al., 1994) would lead to reaching threshold for maintaining the activated state at different times. A fascinating remaining question is how the cortical state change is mechanistically timed to sensory development (e.g., eye opening).

Despite a developmental correlation between low KCC2 expression and delta brushes in humans and rats (Vanhatalo et al., 2005), in both visual and barrel cortex (Minlebaev et al., 2007), their production does not require excitatory GABA. In fact, $GABA_A$ synaptic currents appeared largely inhibitory both before and after the switch. Subplate neurons are critical for the development of visual cortex inhibition, and drive beta-oscillations in isolated neonatal rodent somatosensory cortex (Kanold and Luhmann, 2010), suggesting their possible importance in the response switch. However, our data provide no evidence for this hypothesis. MUA in L6B was not grossly different from other L5–6 units, and we did not observe spiking in white matter (data not shown). Furthermore, in somatosensory slices, cholinergic driven beta-oscillation activity becomes independent of subplate 4 to 5 days before our switch (Dupont et al., 2006), suggesting an independence of the two events.

Primitive Visual Response—Homology and Function

Early cortical light responses consist of three unique components, each with its own network mechanism, but developmentally regulated as a single unit (Figure 10C). The initial component is a ''gamma-burst'' oscillation in L4. Based on their CSD profile (Molnár et al., 2003), failure of cortical diazepam to modify their frequency, and their elimination and replacement by a single potential during optic nerve stimulation, we suggest that the gamma oscillations are the result of weak and poorly timed retinal activity driving oscillations in thalamic relay cells. This summating input then ignites a collective burst that engages all cortical layers. Similar bursts occur spontaneously at the same ages in cortical slices (Rheims et al., 2008) and after eye removal in vivo (Colonnese and Khazipov, 2010), suggesting they are an intrinsic cortical activity. This is further supported by the fact that burst occurrence is dependent on the cortical inhibitory-excitatory balance. Finally, columnar bursts were followed at variable latency (100–500 ms) by delta brush oscillations. Delta brushes are self-organized population events composed of glutamatergic and GABAergic synaptic currents (Minlebaev et al., 2007), though their generative mechanisms are still unclear. In terms of characteristic frequencies, depth profile, and synaptic currents they are remarkably similar between primary limb cortex (Khazipov et al., 2004; Marcano-Reik and Blumberg, 2008), barrel cortex (Minlebaev et al., 2007, 2009; Yang et al., 2009) and visual cortex during the first and second postnatal weeks, where they occur in response to retinal waves (Hanganu et al., 2006; Colonnese and Khazipov, 2010). However, light evoked delta-brushes are not the result of triggered retinal waves, as they were present when activity in the retina was blocked.

The homology between human and rat delta brushes is supported by their similar frequency characteristics, developmental time of expression, and stimulation by sensory input (Khazipov and Luhmann, 2006). The earliest studies of the flash-evoked potential described slow waves with a long delay and a ''rhythmic after-discharge'' (Ellingson, 1960; Hrbek, 1969; Hrbek et al., 1973), but these are the exception, and the extent to which early visual responses are amplified by cortical network properties to produce the complex of activity patterns we describe has been largely overlooked in humans and animals. This is due to a number of experimental factors including the use of anesthesia, low interstimulus intervals (>0.2 Hz), high-pass filtering, and examination of only short-latency responses. By correcting the technical issues and consciously examining rats and preterm infants under similar conditions, we have developed an animal model to study the network basis of visual development in humans. Our data require a re-evaluation of how such data have previously been interpreted. A guiding principle of developmental electrophysiology has been that the long-latency ''nonspecific'' negative potentials of the VEP develop first, and that specific responses develop later. This is based on the

assumption that the negative waves observed in preterm infant VEPs are equivalent to similarly placed potentials in the adult potentials (Hrbek, 1969; Pike et al., 1999; Tsuneishi and Casaer, 1997). Our data suggest that they are not equivalent, however, and that the first negative potential recorded at the cortical surface results from the columnar discharge (which is the only part of the initial response to reach the surface in rats [Figure 4A]) that is part of the immature thalamic input. Later negative potentials likely result from filtering distortions of the evoked delta brush. Thus, our results have important implications for the design of tests of sensory and cortical function in this fragile population.

By showing that visual input produces the same cortical network oscillations as spontaneous retinal waves, we predict that early visual responses should engage similar synaptic plasticity mechanisms and therefore cannot be ignored in models of visual development. In humans, light levels within ranges normally experienced by the mother can trigger fetal movements, heart rate changes, and cortical responses measured by magnetoencephalography or magnetic resonance imaging (Eswaran et al., 2004; Fulford et al., 2003; Peleg and Goldman, 1980; Polishuk et al., 1975). Dark rearing before eye opening disrupts the development of on-off responses in ferret thalamus (Akerman et al., 2002). There are two reasons to believe that early visual responses may play a larger role in primates than in rodents and carnivores. First, while spontaneous retinal waves in rats drive 90% of cortical activity during the bursting period (Colonnese and Khazipov, 2010), macaque retinas show a significant decrease in spontaneous retinal activity during the same developmental stages (Warland et al., 2006). Second, the period of primitive vision occupies a larger portion of gestation in humans than in rats: 12% of the time between conception and the time of the switch in rats, but almost 30% of the same time-frame in humans. Thus, current data predict that the human fetus transitions through an extended period when little coordinated activity is generated spontaneously by the retina but can potentially be induced by light.

The close correlation of the switch in visual responses with eye opening in rodents but birth in humans raises a number of important questions. For instance, did delayed eye opening in altricial animals evolve to prevent light induced oscillations from synchronizing the activity in the two eyes and disrupting eye specific segregation? And vice versa, should preterm babies be kept in visual environments mimicking low-light conditions in utero, in keeping with observations that the premature population has visual acuity and contrast sensitivity deficits not attributable to detectable cerebral lesions or retinopathies (O'Connor et al., 2004)? The determination of well-identified electrical signatures of light responses provided by the present study will facilitate the study of these issues.

EXPERIMENTAL PROCEDURES

Preterm Infants

Human preterm infants at low neurological risk were studied at the neonatal intensive care unit at Cochin-Port Royal Hospital (Paris, France) in accordance with the Code of Ethics of the World Medical Association, and approved by the ethics committee at INSERM. Informed written consent was obtained from all parents. Neurological examinations and transcranial ultrasonography were normal in all infants, who had no history of infection or perinatal asphyxia. Gestational age was calculated postamenorrhea. Care and recording was as described (Milh et al., 2007). Infants were video monitored and light intensity measured with a photometer placed near the head. While resting in low light (1–4 lm m^{-2}), at least 20 manually triggered 100 ms indirect light flashes with a minimal interval of 10 s gave 100 lm m^{-2} maximum near the head (one-half the intensity of normal neonatal ward lighting). The light was calibrated so as not to awaken the child. Before analysis the EEG was analyzed visually by a well-trained neurophysiologist and was considered as age normal. Signals were amplified (1000×), filtered at 0.05 to 97 Hz band pass, acquired at 256 Hz using the Deltamed system, and analyzed offline using the Coherence 3NT program (Deltamed, Paris, France), the open source software EEGlab (Delorme and Makeig, 2004), Matlab (Mathworks, Natick, MA), and Chronux (http://chronux.org [Mitra and Bokil, 2007]) as described in the results and Supplemental Experimental Procedures.

Neonatal Rats

Neonatal rat experiments were in accordance with INSERM and NIH guidelines for the care of animals in research and were approved by the local review committee. We used Wistar rats for correspondence with previous experiments and to mimic the more translucent human eyelid. Experiments at critical time points were performed with Long-Evans rats which were identical to the albino rats (n = 10; see Figure 2). Example traces and data from LE rats are seen in Figures 6 and 7. Recording techniques have been extensively presented (Colonnese and Khazipov, 2010). Body temperature was maintained between 35°C and 36°C. Movement was detected with a piezoelectric device placed under the thorax, and in a subset of animals via nuchal EMG. V1 recordings were localized at 2.8–3.2 mm lateral to midline, and 0.0–0.5 rostral to lambda. In the dark, light flashes were provided every 30 s by green LED (3.4 cd with 35°C) placed 0.5 cm from the contralateral eye. Extracellular recordings were made either with pulled glass microelectrodes (1–2 MΩ) coupled to a direct-current amplifier (Axon Instruments), or multisite linear array Michigan Probes (Neuronexus Tech) coupled to a custom amplifier (A. Alexeev, Trinity, Russia). Frequencies below 1–2 Hz were poorly transmitted by the Michigan Probes and our amplifier; therefore, all multielectrode recordings were high-pass filtered at 2 Hz. All recordings were amplified 1000×, recorded in Axoscope and analyzed with Clampfit (Axon Laboratories) and Matlab as described in Results and Supplemental Experimental Procedures.

SUPPLEMENTAL INFORMATION

Supplemental Information include six figures, one table, one movie, and Supplemental Experimental Procedures and can be found with this article online at doi:10.1016/j.neuron.2010.07.015.

ACKNOWLEDGMENTS

This work was supported by grants from ANR and FRM (R.K., A.K., C.C., Y.B.-A.) and NEI/NIH (EY016966 to M.T.C.). We thank Mms. Florence Thai and Marguerite Barclay for their assistance recording the human infants and Gyorgy Buzsaki, Alain Destexhe, Marla Feller, Marnie Phillips, and Anton Sirota for comments on the manuscript.

Accepted: July 2, 2010
Published: August 11, 2010

REFERENCES

Akerman, C.J., Smyth, D., and Thompson, I.D. (2002). Visual experience before eye opening and the development of the retinogeniculate pathway. Neuron *36*, 869–879.

Amzica, F., and Steriade, M. (1998). Cellular substrates and laminar profile of sleep K-complex. Neuroscience *82*, 671–686.

André, M., Lamblin, M.D., d'Allest, A.M., Curzi-Dascalova, L., Moussalli-Salefranque, F., Nguyen The Tich, S., Vecchierini-Blineau, M.F., Wallois, F., Walls-Esquivel, E., and Plouin, P. (2010). Electroencephalography in premature

and full-term infants. Developmental features and glossary. Neurophysiol. Clin. *40*, 59–124.

Ben-Ari, Y., Gaiarsa, J.L., Tyzio, R., and Khazipov, R. (2007). GABA: a pioneer transmitter that excites immature neurons and generates primitive oscillations. Physiol. Rev. *87*, 1215–1284.

Berridge, C.W., and Waterhouse, B.D. (2003). The locus coeruleus-noradrenergic system: modulation of behavioral state and state-dependent cognitive processes. Brain Res. Brain Res. Rev. *42*, 33–84.

Birch, E.E., and Stager, D.R. (1996). The critical period for surgical treatment of dense congenital unilateral cataract. Invest. Ophthalmol. Vis. Sci. *37*, 1532–1538.

Burkhalter, A., Bernardo, K.L., and Charles, V. (1993). Development of local circuits in human visual cortex. J. Neurosci. *13*, 1916–1931.

Butts, D.A., Kanold, P.O., and Shatz, C.J. (2007). A burst-based "Hebbian" learning rule at retinogeniculate synapses links retinal waves to activity-dependent refinement. PLoS Biol. *5*, e61.. 10.1371/journal.pbio.0050061.

Callaway, E.M., and Katz, L.C. (1990). Emergence and refinement of clustered horizontal connections in cat striate cortex. J. Neurosci. *10*, 1134–1153.

Chapman, B., and Stryker, M.P. (1993). Development of orientation selectivity in ferret visual cortex and effects of deprivation. J. Neurosci. *13*, 5251–5262.

Chiu, C., and Weliky, M. (2001). Spontaneous activity in developing ferret visual cortex in vivo. J. Neurosci. *21*, 8906–8914.

Colonnese, M.T., and Khazipov, R. (2010). "Slow activity transients" in infant rat visual cortex: a spreading synchronous oscillation patterned by retinal waves. J. Neurosci. *30*, 4325–4337.

Contreras, D., Destexhe, A., Sejnowski, T.J., and Steriade, M. (1996). Control of spatiotemporal coherence of a thalamic oscillation by corticothalamic feedback. Science *274*, 771–774.

Contreras, D., Destexhe, A., Sejnowski, T.J., and Steriade, M. (1997). Spatiotemporal patterns of spindle oscillations in cortex and thalamus. J. Neurosci. *17*, 1179–1196.

Daw, M.I., Ashby, M.C., and Isaac, J.T.R. (2007). Coordinated developmental recruitment of latent fast spiking interneurons in layer IV barrel cortex. Nat. Neurosci. *10*, 453–461.

Delorme, A., and Makeig, S. (2004). EEGLAB: an open source toolbox for analysis of single-trial EEG dynamics including independent component analysis. J. Neurosci. Methods *134*, 9–21.

Demas, J., Eglen, S.J., and Wong, R.O.L. (2003). Developmental loss of synchronous spontaneous activity in the mouse retina is independent of visual experience. J. Neurosci. *23*, 2851–2860.

Dreyfus-Brisac, C., and Monod, N. (1965). Sleep of premature and full-term neonates—a polygraphic study. Proc. R. Soc. Med. *58*, 6–7.

Dupont, E., Hanganu, I.L., Kilb, W., Hirsch, S., and Luhmann, H.J. (2006). Rapid developmental switch in the mechanisms driving early cortical columnar networks. Nature *439*, 79–83.

Durack, J.C., and Katz, L.C. (1996). Development of horizontal projections in layer 2/3 of ferret visual cortex. Cereb. Cortex *6*, 178–183.

Dzhala, V.I., Talos, D.M., Sdrulla, D.A., Brumback, A.C., Mathews, G.C., Benke, T.A., Delpire, E., Jensen, F.E., and Staley, K.J. (2005). NKCC1 transporter facilitates seizures in the developing brain. Nat. Med. *11*, 1205–1213.

Ellingson, R.J. (1960). Cortical electrical responses to visual stimulation in the human infant. Electroencephalogr. Clin. Neurophysiol. *12*, 663–677.

Ellingson, R.J. (1970). Variability of visual evoked responses in the human newborn. Electroencephalogr. Clin. Neurophysiol. *29*, 10–19.

Eswaran, H., Lowery, C.L., Wilson, J.D., Murphy, P., and Preissl, H. (2004). Functional development of the visual system in human fetus using magnetoencephalography. Exp. Neurol. *190* (*Suppl 1*), S52–S58.

Evrard, A., and Ropert, N. (2009). Early development of the thalamic inhibitory feedback loop in the primary somatosensory system of the newborn mice. J. Neurosci. *29*, 9930–9940.

Fagiolini, M., Pizzorusso, T., Berardi, N., Domenici, L., and Maffei, L. (1994). Functional postnatal development of the rat primary visual cortex and the role of visual experience: dark rearing and monocular deprivation. Vision Res. *34*, 709–720.

Finlay, B.L., and Darlington, R.B. (1995). Linked regularities in the development and evolution of mammalian brains. Science *268*, 1578–1584.

Foote, S.L., and Morrison, J.H. (1987). Extrathalamic modulation of cortical function. Annu. Rev. Neurosci. *10*, 67–95.

Frank, M.G., and Heller, H.C. (2003). The ontogeny of mammalian sleep: a reappraisal of alternative hypotheses. J. Sleep Res. *12*, 25–34.

Fulford, J., Vadeyar, S.H., Dodampahala, S.H., Moore, R.J., Young, P., Baker, P.N., James, D.K., and Gowland, P.A. (2003). Fetal brain activity in response to a visual stimulus. Hum. Brain Mapp. *20*, 239–245.

Galuske, R.A., and Singer, W. (1996). The origin and topography of long-range intrinsic projections in cat visual cortex: a developmental study. Cereb. Cortex *6*, 417–430.

Golshani, P., Gonçalves, J.T., Khoshkhoo, S., Mostany, R., Smirnakis, S., and Portera-Cailliau, C. (2009). Internally mediated developmental desynchronization of neocortical network activity. J. Neurosci. *29*, 10890–10899.

Hanganu, I.L., Ben-Ari, Y., and Khazipov, R. (2006). Retinal waves trigger spindle bursts in the neonatal rat visual cortex. J. Neurosci. *26*, 6728–6736.

Hanganu, I.L., Staiger, J.F., Ben-Ari, Y., and Khazipov, R. (2007). Cholinergic modulation of spindle bursts in the neonatal rat visual cortex in vivo. J. Neurosci. *27*, 5694–5705.

Hasenstaub, A., Sachdev, R.N.S., and McCormick, D.A. (2007). State changes rapidly modulate cortical neuronal responsiveness. J. Neurosci. *27*, 9607–9622.

Hrbek, A. (1969). Visual evoked responses in the newborn infant. Int. Ophthalmol. Clin. *9*, 1051–1072.

Hrbek, A., Karlberg, P., and Olsson, T. (1973). Development of visual and somatosensory evoked responses in pre-term newborn infants. Electroencephalogr. Clin. Neurophysiol. *34*, 225–232.

Huang, Z.J., Kirkwood, A., Pizzorusso, T., Porciatti, V., Morales, B., Bear, M.F., Maffei, L., and Tonegawa, S. (1999). BDNF regulates the maturation of inhibition and the critical period of plasticity in mouse visual cortex. Cell *98*, 739–755.

Huberman, A.D., Feller, M.B., and Chapman, B. (2008). Mechanisms underlying development of visual maps and receptive fields. Annu. Rev. Neurosci. *31*, 479–509.

Johnston, M.V., and Coyle, J.T. (1981). Development of central neurotransmitter systems. Ciba Found. Symp. *86*, 251–270.

Jouvet-Mounier, D., Astic, L., and Lacote, D. (1970). Ontogenesis of the states of sleep in rat, cat, and guinea pig during the first postnatal month. Dev. Psychobiol. *2*, 216–239.

Kanold, P.O., and Luhmann, H.J. (2010). The subplate and early cortical circuits. Annu. Rev. Neurosci. *33*, 23–48.

Karlsson, K.A.E., Gall, A.J., Mohns, E.J., Seelke, A.M.H., and Blumberg, M.S. (2005). The neural substrates of infant sleep in rats. PLoS Biol. *3*, e143.. 10.1371/journal.pbio.0030143.

Katz, L.C., and Shatz, C.J. (1996). Synaptic activity and the construction of cortical circuits. Science *274*, 1133–1138.

Khazipov, R., and Luhmann, H.J. (2006). Early patterns of electrical activity in the developing cerebral cortex of humans and rodents. Trends Neurosci. *29*, 414–418.

Khazipov, R., Sirota, A., Leinekugel, X., Holmes, G.L., Ben-Ari, Y., and Buzsáki, G. (2004). Early motor activity drives spindle bursts in the developing somatosensory cortex. Nature *432*, 758–761.

Kraemer, M., Abrahamsson, M., and Sjöström, A. (1999). The neonatal development of the light flash visual evoked potential. Doc. Ophthalmol. *99*, 21–39.

Krug, K., Akerman, C.J., and Thompson, I.D. (2001). Responses of neurons in neonatal cortex and thalamus to patterned visual stimulation through the naturally closed lids. J. Neurophysiol. *85*, 1436–1443.

Landers, M., and Philip Zeigler, H. (2006). Development of rodent whisking: trigeminal input and central pattern generation. Somatosens. Mot. Res. *23*, 1–10.

Latsari, M., Dori, I., Antonopoulos, J., Chiotelli, M., and Dinopoulos, A. (2002). Noradrenergic innervation of the developing and mature visual and motor cortex of the rat brain: a light and electron microscopic immunocytochemical analysis. J. Comp. Neurol. *445*, 145–158.

Li, Y., Van Hooser, S.D., Mazurek, M., White, L.E., and Fitzpatrick, D. (2008). Experience with moving visual stimuli drives the early development of cortical direction selectivity. Nature *456*, 952–956.

Long, M.A., Cruikshank, S.J., Jutras, M.J., and Connors, B.W. (2005). Abrupt maturation of a spike-synchronizing mechanism in neocortex. J. Neurosci. *25*, 7309–7316.

Lu, W., and Constantine-Paton, M. (2004). Eye opening rapidly induces synaptic potentiation and refinement. Neuron *43*, 237–249.

Marcano-Reik, A.J., and Blumberg, M.S. (2008). The corpus callosum modulates spindle-burst activity within homotopic regions of somatosensory cortex in newborn rats. Eur. J. Neurosci. *28*, 1457–1466.

McCormick, D.A., Trent, F., and Ramoa, A.S. (1995). Postnatal development of synchronized network oscillations in the ferret dorsal lateral geniculate and perigeniculate nuclei. J. Neurosci. *15*, 5739–5752.

Mechawar, N., and Descarries, L. (2001). The cholinergic innervation develops early and rapidly in the rat cerebral cortex: a quantitative immunocytochemical study. Neuroscience *108*, 555–567.

Milh, M., Kaminska, A., Huon, C., Lapillonne, A., Ben-Ari, Y., and Khazipov, R. (2007). Rapid cortical oscillations and early motor activity in premature human neonate. Cereb. Cortex *17*, 1582–1594.

Minlebaev, M., Ben-Ari, Y., and Khazipov, R. (2007). Network mechanisms of spindle-burst oscillations in the neonatal rat barrel cortex in vivo. J. Neurophysiol. *97*, 692–700.

Minlebaev, M., Ben-Ari, Y., and Khazipov, R. (2009). NMDA receptors pattern early activity in the developing barrel cortex in vivo. Cereb. Cortex *19*, 688–696.

Mitra, P., and Bokil, H. (2007). Observed Brain Dynamics, First Edition (Oxford: Oxford University Press).

Mitzdorf, U. (1985). Current source-density method and application in cat cerebral cortex: investigation of evoked potentials and EEG phenomena. Physiol. Rev. *65*, 37–100.

Molnár, Z., Kurotani, T., Higashi, S., Yamamoto, N., and Toyama, K. (2003). Development of functional thalamocortical synapses studied with current source-density analysis in whole forebrain slices in the rat. Brain Res. Bull. *60*, 355–371.

O'Connor, A.R., Stephenson, T.J., Johnson, A., Tobin, M.J., Ratib, S., Moseley, M., and Fielder, A.R. (2004). Visual function in low birthweight children. Br. J. Ophthalmol. *88*, 1149–1153.

Ohshiro, T., and Weliky, M. (2006). Simple fall-off pattern of correlated neural activity in the developing lateral geniculate nucleus. Nat. Neurosci. *9*, 1541–1548.

Peleg, D., and Goldman, J.A. (1980). Fetal heart rate acceleration in response to light stimulation as a clinical measure of fetal well-being. A preliminary report. J. Perinat. Med. *8*, 38–41.

Petersen, C.C.H., Hahn, T.T.G., Mehta, M., Grinvald, A., and Sakmann, B. (2003). Interaction of sensory responses with spontaneous depolarization in layer 2/3 barrel cortex. Proc. Natl. Acad. Sci. USA *100*, 13638–13643.

Pike, A.A., Marlow, N., and Reber, C. (1999). Maturation of the flash visual evoked potential in preterm infants. Early Hum. Dev. *54*, 215–222.

Polishuk, W.Z., Laufer, N., and Sadovsky, E. (1975). Fetal reaction to external light. Harefuah *89*, 395–396.

Quinlan, E.M., Philpot, B.D., Huganir, R.L., and Bear, M.F. (1999). Rapid, experience-dependent expression of synaptic NMDA receptors in visual cortex in vivo. Nat. Neurosci. *2*, 352–357.

Rakic, P. (1976). Prenatal genesis of connections subserving ocular dominance in the rhesus monkey. Nature *261*, 467–471.

Rakic, P., Bourgeois, J.P., and Goldman-Rakic, P.S. (1994). Synaptic development of the cerebral cortex: implications for learning, memory, and mental illness. Prog. Brain Res. *102*, 227–243.

Rheims, S., Minlebaev, M., Ivanov, A., Represa, A., Khazipov, R., Holmes, G.L., Ben-Ari, Y., and Zilberter, Y. (2008). Excitatory GABA in rodent developing neocortex in vitro. J. Neurophysiol. *100*, 609–619.

Robertson, R.T., Tijerina, A.A., and Gallivan, M.E. (1985). Transient patterns of acetylcholinesterase activity in visual cortex of the rat: normal development and the effects of neonatal monocular enucleation. Brain Res. *353*, 203–214.

Rochefort, N.L., Garaschuk, O., Milos, R.I., Narushima, M., Marandi, N., Pichler, B., Kovalchuk, Y., and Konnerth, A. (2009). Sparsification of neuronal activity in the visual cortex at eye opening. Proc. Natl. Acad. Sci. USA *106*, 15049–15054.

Ruthazer, E.S., and Stryker, M.P. (1996). The role of activity in the development of long-range horizontal connections in area 17 of the ferret. J. Neurosci. *16*, 7253–7269.

Sachdev, R.N.S., Ebner, F.F., and Wilson, C.J. (2004). Effect of subthreshold up and down states on the whisker-evoked response in somatosensory cortex. J. Neurophysiol. *92*, 3511–3521.

Salapatek, P. (1986). Handbook of Infant Perception: From Sensation to Perception (San Diego, CA: Academic Press).

Sanchez-Vives, M.V., and McCormick, D.A. (2000). Cellular and network mechanisms of rhythmic recurrent activity in neocortex. Nat. Neurosci. *3*, 1027–1034.

Seelke, A.M.H., and Blumberg, M.S. (2010). Developmental appearance and disappearance of cortical events and oscillations in infant rats. Brain Res. *1324*, 34–42.

Sherman, S.M., and Guillery, R.W. (2009). Exploring the Thalamus and Its Role in Cortical Function, Second Edition (Cambridge, MA: The MIT Press).

Shu, Y., Hasenstaub, A., and McCormick, D.A. (2003). Turning on and off recurrent balanced cortical activity. Nature *423*, 288–293.

Sipilä, S.T., Schuchmann, S., Voipio, J., Yamada, J., and Kaila, K. (2006). The cation-chloride cotransporter NKCC1 promotes sharp waves in the neonatal rat hippocampus. J. Physiol. *573*, 765–773.

Smith, S.L., and Trachtenberg, J.T. (2007). Experience-dependent binocular competition in the visual cortex begins at eye opening. Nat. Neurosci. *10*, 370–375.

Steriade, M., and McCarley, R.W. (2005). Brain Control of Wakefulness and Sleep (New York: Springer).

Swadlow, H.A., Gusev, A.G., and Bezdudnaya, T. (2002). Activation of a cortical column by a thalamocortical impulse. J. Neurosci. *22*, 7766–7773.

Tian, N., and Copenhagen, D.R. (2003). Visual stimulation is required for refinement of ON and OFF pathways in postnatal retina. Neuron *39*, 85–96.

Timofeev, I., Grenier, F., Bazhenov, M., Sejnowski, T.J., and Steriade, M. (2000). Origin of slow cortical oscillations in deafferented cortical slabs. Cereb. Cortex *10*, 1185–1199.

Tolonen, M., Palva, J.M., Andersson, S., and Vanhatalo, S. (2007). Development of the spontaneous activity transients and ongoing cortical activity in human preterm babies. Neuroscience *145*, 997–1006.

Tsuneishi, S., and Casaer, P. (1997). Stepwise decrease in VEP latencies and the process of myelination in the human visual pathway. Brain Dev. *19*, 547–551.

Tyzio, R., Cossart, R., Khalilov, I., Minlebaev, M., Hübner, C.A., Represa, A., Ben-Ari, Y., and Khazipov, R. (2006). Maternal oxytocin triggers a transient inhibitory switch in GABA signaling in the fetal brain during delivery. Science *314*, 1788–1792.

Vanhatalo, S., Palva, J.M., Andersson, S., Rivera, C., Voipio, J., and Kaila, K. (2005). Slow endogenous activity transients and developmental expression of K+-Cl- cotransporter 2 in the immature human cortex. Eur. J. Neurosci. *22*, 2799–2804.

Venkatesan, C., Song, X.Z., Go, C.G., Kurose, H., and Aoki, C. (1996). Cellular and subcellular distribution of alpha 2A-adrenergic receptors in the visual cortex of neonatal and adult rats. J. Comp. Neurol. *365*, 79–95.

Warland, D.K., Huberman, A.D., and Chalupa, L.M. (2006). Dynamics of spontaneous activity in the fetal macaque retina during development of retinogeniculate pathways. J. Neurosci. *26*, 5190–5197.

Warren, R.A., Agmon, A., and Jones, E.G. (1994). Oscillatory synaptic interactions between ventroposterior and reticular neurons in mouse thalamus in vitro. J. Neurophysiol. *72*, 1993–2003.

Weliky, M., and Katz, L.C. (1999). Correlational structure of spontaneous neuronal activity in the developing lateral geniculate nucleus in vivo. Science *285*, 599–604.

White, L.E., Coppola, D.M., and Fitzpatrick, D. (2001). The contribution of sensory experience to the maturation of orientation selectivity in ferret visual cortex. Nature *411*, 1049–1052.

Wong, R.O., Meister, M., and Shatz, C.J. (1993). Transient period of correlated bursting activity during development of the mammalian retina. Neuron *11*, 923–938.

Yamada, J., Okabe, A., Toyoda, H., Kilb, W., Luhmann, H.J., and Fukuda, A. (2004). Cl^- uptake promoting depolarizing GABA actions in immature rat neocortical neurones is mediated by NKCC1. J. Physiol. *557*, 829–841.

Yang, J.W., Hanganu-Opatz, I.L., Sun, J.J., and Luhmann, H.J. (2009). Three patterns of oscillatory activity differentially synchronize developing neocortical networks in vivo. J. Neurosci. *29*, 9011–9025.